

REVIEW ARTICLE

# An examination of the formation and characteristics of charge-density waves in inorganic materials with special reference to the two- and one-dimensional transition-metal chalcogenides

To cite this article: R L Withers and J A Wilson 1986 *J. Phys. C: Solid State Phys.* **19** 4809

View the [article online](#) for updates and enhancements.

## You may also like

- [Structural stability of coplanar 1T-2H superlattice MoS<sub>2</sub> under high energy electron beam](#)  
S Reshmi, M V Akshaya, Biswarup Satpati et al.
- [Unconventional thermal transport enhancement with large atom mass: a comparative study of 2D transition dichalcogenides](#)  
Huimin Wang, Guangzhao Qin, Guojian Li et al.
- [Two-dimensional MoS<sub>2</sub> electromechanical actuators](#)  
Nguyen T Hung, Ahmad R T Nugraha and Riichiro Saito

## REVIEW ARTICLE

# An examination of the formation and characteristics of charge-density waves in inorganic materials with special reference to the two- and one-dimensional transition-metal chalcogenides

R L Withers† and J A Wilson

H H Wills Physics Laboratory, University of Bristol, BS8 1TL, UK

Received 16 December 1985

**Abstract.** We have attempted to provide a relatively brief outline of the current situation regarding the formation and properties of charge density wave states in low-dimensional transition metal compounds. Because we believe that to make further progress at this stage the details of the situation must be looked to with greater attention, we have chosen to illustrate the types of problem involved by specifically focusing on 1T- and 2H-TaS<sub>2</sub> and TaSe<sub>2</sub>, VSe<sub>2</sub>, NbSe<sub>3</sub> and NbTe<sub>4</sub>, where our own research has centred.

In §2 we provide a survey of the theory of CDW/PLD formation, indicating where the approximations lie. The fact that low-dimensional compounds are open to low energy-cost distortions is emphasised. Pressure or intercalation invariably suppresses  $T_0$ .

In §3 we introduce the transition metal chalcogenides, from the early electron microscopy through to recent scanning tunnelling imaging of the CDW/PLD.

With this background the first three parts of §4 present the evidence for the relative roles played by the non-interacting electronic susceptibility  $\chi^0(q)$ , the dressed susceptibility  $\chi(q)$  (especially as affected by electron–phonon coupling), and the more general band structural considerations. It is soon evident that the energy balances selecting one mode of distortion and CDW phasing over another are very marginal in 2D compounds. It is not yet possible to calculate with any certainty even whether a system becomes unstable within a simple harmonic framework or requires anharmonic mode–mode coupling.

A look at the pretransitional states is provided in §5. The observed diffuse scattering comes from impurity-seeded SRO as well as intrinsic SRO. Below  $T_0$  diffuse scattering can persist through the phason scattering of the CDW.

In §6 the static CDW states are investigated particularly with regard to discommensuration formation and detection. The inadequacies of simple Landau theory are highlighted.

We hope with this paper to have set the more interesting recent research on these systems in perspective. Clearly the work is at the end of the beginning, yet, equally clearly, far from the beginning of the end.

We have chosen not to deal with CDW sliding since the dynamics of CDW have received much attention of late. However, until the detailed form and origin of the microstructure of CDW states is finally recognised, much of what is said about sliding must be inadequate.

Discussion of TiSe<sub>2</sub> has been deferred to a subsequent work.

New areas like the effects of magnetic fields on CDW are emerging, and the number of metals (as of insulators) with incommensurate states continues to rise steadily. We await application of this new physics with interest.

† Present address: Research School of Chemistry, Australian National University, GPO Box 4, Canberra ACT 2601, Australia.

## 1. Introduction

Prior to the 1970s charge-density waves and their concomitant periodic structural distortions were subjects for theoretical debate only. Then, with the advent of the investigation of the low-dimensional inorganic metallic compounds  $\text{TaSe}_2$  and  $\text{K}_2\text{Pt}(\text{CN})_4 \cdot \text{O} \cdot 3\text{Br} \cdot n\text{H}_2\text{O}$  (i.e. KCP), followed by organics like TTF-TCNQ, it became known that these phenomena do actually exist. Elaboration of what the basic phenomena were took most of the remainder of the decade. These endeavours, besides supplying excellent working materials for new experimental and theoretical methods such as XPS, ARPES and TDPAC, and band-structure and  $\chi^o(q)$  calculations, also led investigators to the realisation that many more materials than at first were suspected are able to support CDWs (charge-density waves), e.g.  $\text{TiSe}_2$ ,  $\text{NbSe}_3$ ,  $\text{NbTe}_4$ ,  $\text{Mo}_2\text{S}_3$ ,  $\text{Nb}_3\text{Te}_4$ ,  $\text{K}_{0.3}\text{MoO}_3$ ,  $\text{Mo}_4\text{O}_{11}$ ,  $(\text{TaSe}_4)_2\text{I}$ ,  $\text{CuS}_2$ ,  $\text{CuV}_2\text{S}_4$ , plus a host of organics, and even the  $\alpha$ -form of elementary uranium.

In as far as many of these materials acquire distortions that are in some temperature range incommensurate with the basic lattice, they form part of a wider field of interest that has developed in incommensurate structures. The latter may arise with insulators (such as quartz,  $\text{NaNO}_2$ ,  $\text{ThBr}_4$  and thio-urea) or magnetics (such as  $\text{NiBr}_2$ ,  $\text{CeSb}$  and  $\text{Pr}$ ), or in alloy ordering and anti-phase boundaries (as for  $\text{Ag/Cd}$ ,  $\text{Cu/Sb}$  or  $\text{Cu/Pd}$ ). In each case there has naturally been much questioning as to what drives the phenomena, and what determines amplitudes, wave-vectors and the various other characteristics. With regard to CDW materials, and to metallic alloy MDWs, and to SDWs, it always has been recognised that Fermi surface nesting in one way or another plays a vital role. In this Article we will observe for selected transition-metal layer and chain chalcogenides how electron–phonon coupling lies at the heart of the response, as was outlined in Chan and Heine's pioneering theoretical work.

The theoretical work of McMillan foresaw also how strong electron–phonon coupling might lead to a discommensurate rather than a uniformly incommensurate state. Such discommensuration arrays were not observed until the 1980s. Indeed the CDW field has now entered a new era of experimental and theoretical sophistication—the detailed examination of microstructures, the coupling between CDWs and superconductivity, CDW formation in magnetic fields (e.g. in graphite at 25 T), supersymmetry, fractal and multi-term Landau theories. Perhaps nothing has caught the general attention so much as CDW sliding in  $\text{NbSe}_3$  and related materials under RF or small DC fields. Because so much has now been written about CDW dynamics we will not encroach upon this topic (see, for example, Monceau 1985, Wilson 1985a). Instead, we will concentrate upon the primary formation of CDW/PLDs (periodic lattice distortions), with a few comments on the way in which mechanical, thermal, electrical and magnetic properties bear witness to the seat and nature of their origin. In particular we stress the need for a thorough understanding and appreciation of the structural complexities of each system. Nowhere does use of the electron microscope show up to better advantage than in revealing the structural complexities developed—witness the unexpected orthorhombic domains, the discommensuration arrays and the stripe phase in 2H-TaSe<sub>2</sub>, the 2q-behaviour of VSe<sub>2</sub>, the doping characteristics for 1T-TaS<sub>2</sub>, and the CDW defect microstructure of NbSe<sub>3</sub>. One is able in addition to examine the scattering from SRO present at temperatures above onset, or again to determine the space group of a commensurate phase below lock-in, or in a favourable case to go on to establish the full superlattice structure. Given such structural information the way is now open for a bold practitioner in modern, self-consistent, fully relativistic band-structure methods to contemplate calculating total energies for the

various structural possibilities—a stage beyond calculating relative stabilities for normal allotropes like graphite versus diamond.

As yet we await some ingenious application of this new physics. Whether or not CDWS can follow in the steps of liquid crystals, that other boom topic of the 1970s, they certainly add a further chapter in our understanding of matter.

## 2. Basic theory of CDW/PLD instabilities

The relationship between the Fermi surface, CDWs, and the existence of phonon softening in transition-metal compounds has had a rather confusing history. The initial suggestion that the electronic energy of a metal could be lowered by a CDW was first put forward by Peierls (1955) and Fröhlich (1954). They considered the special case of a one-dimensional metal, the Fermi surface for which consists of two parallel planes. Since then numerous authors (Overhauser 1962, Halperin and Rice 1968, Chan and Heine 1973, . . .) have considered the instabilities that may result from such strong nesting (quasi-one-dimensional) situations.

A self-consistent periodic potential for which the wave-vector exactly spans a section of the Fermi surface will couple electronic states across that section of the Fermi surface and involve a static periodic modulation of the conduction electron density, i.e. a CDW. Occupied electron states near the Fermi surface sections in question will have their energy lowered while the corresponding empty states above  $E_F$  have their energy raised (figure 1). Such a periodic modulation of the conduction electron density necessarily is

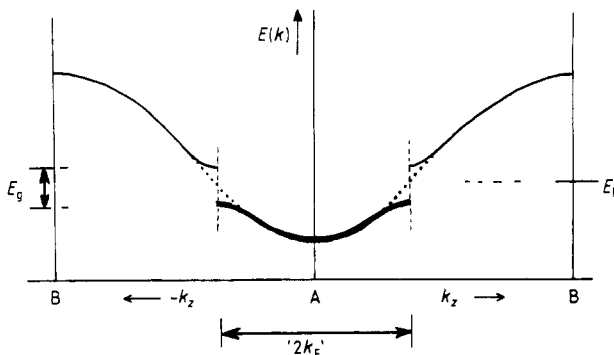


**Figure 1.** The simple one-dimensional case of electronic energy stabilisation in a ' $2k_F$ ' Peierls distortion.

accompanied by a longitudinal modulation of the lattice with identical wave-vector, i.e. by PLD. If the overall change in the total energy, due to changes in the one-electron band-structure energy, the lattice elastic energy and the self-energy of the electrons, is negative, then this coupled CDW/PLD ground state will arise.

Following Cowley (1980; see also Cowley 1978) and others the above balance can be expressed, within the harmonic approximation, in terms of the frequency of that softening normal mode (here labelled by  $j$ ) that eventually is to become the static PLD below some onset transition temperature, via the expression

$$\omega(\mathbf{q}, j)^2 = \omega^B(\mathbf{q}, j)^2 + \sum^E (\mathbf{q}, j). \quad (2.1)$$

Here  $\omega^B(\mathbf{q}, j)^2$  represents the contribution to the energy arising from direct ion-ion core interactions, while  $\Sigma^E(\mathbf{q}, j)$  represents the contribution from the electron energies of states outside the core (consisting of the contribution from their one-electron band-structure energy less than that from their self-energy). In turn

$$\Sigma^E(\mathbf{q}, j) = - \sum_{\mathbf{G}, \mathbf{G}'} g(\mathbf{q} + \mathbf{G}, j) g(-\mathbf{q} - \mathbf{G}', j) \chi^E(-\mathbf{q} - \mathbf{G}, \mathbf{q} + \mathbf{G}') \quad (2.2)$$

where the  $g(\mathbf{q}, j)$  are electron-phonon coupling parameters,  $\mathbf{G}, \mathbf{G}'$  are reciprocal-lattice vectors, and  $\chi^E$  is the generalised electronic susceptibility. The sum over  $\mathbf{G}, \mathbf{G}'$  arises because the change in potential seen by each outer electron with the appearance of the PLD will, in general, contain an infinite series of Fourier coefficients

$$V^{(q)}(\mathbf{r}) = \sum_{\mathbf{G}} V_{\mathbf{G}} \exp[i(\mathbf{q} + \mathbf{G}) \cdot \mathbf{r}].$$

Likewise the self-consistent response of these electrons will also contain an infinite series of Fourier coefficients.

The non-interacting electronic susceptibility, in general, is given by

$$\begin{aligned} \chi^0(-\mathbf{q} - \mathbf{G}, \mathbf{q} + \mathbf{G}') = & - \sum_{\lambda\lambda'} \sum_{\mathbf{k}} \frac{f(\mathbf{k}, \lambda) - f(\mathbf{k} + \mathbf{q}, \lambda')}{\varepsilon(\mathbf{k}, \lambda) - \varepsilon(\mathbf{k} + \mathbf{q}, \lambda')} \\ & \times \langle \mathbf{k}, \lambda | \exp(-i(\mathbf{q} + \mathbf{G}) \cdot \mathbf{r}) | \mathbf{k} + \mathbf{q}, \lambda' \rangle \\ & \times \langle \mathbf{k} + \mathbf{q}, \lambda' | \exp(i(\mathbf{q} + \mathbf{G}') \cdot \mathbf{r}) | \mathbf{k}, \lambda \rangle \end{aligned} \quad (2.3)$$

where the electrons are described by Bloch waves with wave-vector  $\mathbf{k}$ , band index  $\lambda$ , energy  $\varepsilon(\mathbf{k}, \lambda)$  and Fermi occupation number  $f(\mathbf{k}, \lambda)$ .

For the case of nearly free electrons (NFE) the electronic susceptibility  $\chi^E(-\mathbf{q} - \mathbf{G}, \mathbf{q} + \mathbf{G}')$  becomes diagonal in the wave-vector, and  $\chi^E(\mathbf{q} + \mathbf{G})$ , the electronic susceptibility, is now related (see Anderson 1984) to the non-interacting electronic susceptibility  $\chi^0(\mathbf{q} + \mathbf{G})$  by

$$\chi^E(\mathbf{q} + \mathbf{G}) = \chi_0(\mathbf{q} + \mathbf{G}) / (1 + \beta(\mathbf{q} + \mathbf{G}) \chi_0(\mathbf{q} + \mathbf{G})) \quad (2.4)$$

where  $\beta(\mathbf{q} + \mathbf{G})$  is the electron-electron coupling parameter. Thus if we simplify further by ignoring Umklapp processes,  $\Sigma^E(\mathbf{q}, j)$  becomes

$$-|g(\mathbf{q}, j)|^2 \chi^0(\mathbf{q}) / (1 + \beta(\mathbf{q}) \chi^0(\mathbf{q}))$$

and the criterion for CDW/PLD instability from (1.1) becomes

$$[|g(\mathbf{q}, j)|^2 / \omega^B(\mathbf{q}, j)^2] - \beta(\mathbf{q}) > 1 / \chi^0(\mathbf{q}). \quad (2.5)$$

The initial lattice perturbation is considered here to have only one major Fourier coefficient and so the change in potential seen by each electron due to the PLD is given by

$$Q_{\text{PLD}}(\mathbf{q}, j) g(\mathbf{q}, j) e^{i\mathbf{q} \cdot \mathbf{r}}.$$

The non-interacting electronic susceptibility is then given by

$$\chi^0(-\mathbf{q}, \mathbf{q}) \equiv \chi^0(\mathbf{q}) = - \sum_{\lambda\lambda'} \sum_{\mathbf{k}} \frac{f(\mathbf{k}, \lambda) - f(\mathbf{k} + \mathbf{q}, \lambda')}{\varepsilon(\mathbf{k}, \lambda) - \varepsilon(\mathbf{k} + \mathbf{q}, \lambda')} |\langle \mathbf{k}, \lambda | e^{-i\mathbf{q} \cdot \mathbf{r}} | \mathbf{k} + \mathbf{q}, \lambda' \rangle|^2. \quad (2.6)$$

Within a NFE approach it is quite reasonable to assume that the matrix elements in  $\chi^0(\mathbf{q})$

will not be a function of  $\mathbf{k}$  or  $\mathbf{q}$ , although *not* that they will be independent of the choice of  $\lambda$  and  $\lambda'$ . Thus the usual definition of  $\chi^0(\mathbf{q})$ , which simply ignores the matrix elements in (2.6), is misleading when used to give estimates of the overall magnitude of  $\chi^0(\mathbf{q})$ . What is a more reasonable approximation is to consider just intra-conduction-band scattering in definitions of  $\chi^0(\mathbf{q})$ , particularly since a CDW is usually presumed to be purely a conduction electron effect. The Fourier coefficient of the potential that each conduction electron experiences due to the coupled CDW/PLD is then given by

$$v(\mathbf{q}) = g(\mathbf{q}, j)Q_{\text{PLD}}(\mathbf{q}, j) - \beta(\mathbf{q})|\rho_{\text{CDW}}(\mathbf{q})| \quad (2.7)$$

where  $Q_{\text{PLD}}(\mathbf{q}, j)$  and  $\rho_{\text{CDW}}(\mathbf{q})$  are the amplitudes of the PLD and CDW respectively. The uniform band gap thereby opened at the Fermi surface is  $2|v(\mathbf{q})|$ .  $\beta(\mathbf{q})$  is the Fourier coefficient of the electron–electron interaction, which in the Hartree approximation is given by  $e^2/\epsilon_0q^2$ . Littlewood and Heine (1981) include the effects of exchange and correlation by modifying the simple coulombic interaction by a multiplicative factor, so that

$$\beta(\mathbf{q}) = (e^2/\epsilon_0q^2)(1 - f(\mathbf{q})). \quad (2.8)$$

Equation (2.5) above suggests three significant factors that encourage CDW/PLD instabilities. The first is a large non-interacting electronic susceptibility  $\chi^0(\mathbf{q})$ , the second is a large electron–phonon coupling parameter  $g(\mathbf{q}, j)$  and the third is that  $f(\mathbf{q})$  should approach unity as closely as possible in conditions where the exchange and correlation potential limits as far as possible the repulsive coulombic interactions. There are certain conflicts here since high  $\chi^0(\mathbf{q})$  and high  $f(\mathbf{q})$  require narrow bands and high densities of states, while high  $g(\mathbf{q})$  requires broader bands. However, favourable  $\chi^0(\mathbf{q})$  and  $g(\mathbf{q})/\omega^B(\mathbf{q})$  both occur for materials of low dimensionality, as we shall see, and this is precisely where the occurrence of CDW/PLDs is most in evidence.

In the case of the CDW/PLD instabilities in the group V layered transition-metal dichalcogenides (TMDs), where the conduction d electrons are in the tight-binding limit, the NFE approximations are clearly inappropriate. To calculate self-consistently all the various Fourier coefficients is obviously then a difficult task, which within a plane-wave approach would require diagonalising matrices of order several hundred. Varma and Weber (1977, 1979) have recently proposed an extremely successful alternative approach whereby the tight-binding nature of the conduction d-electron wavefunctions is taken into account from the beginning, and the dynamical matrix is calculated from self-consistent changes in Hamiltonian and overlap tight-binding integrals with respect to changes in inter-atomic distances within a non-orthogonal tight-binding (NTB) framework.

The Bloch functions are expanded as:

$$\psi(\mathbf{k}, \lambda) = \frac{1}{N} \sum_{i,m} \varphi_{im}(\mathbf{r}) e^{i\mathbf{k}\cdot\mathbf{R}_i} A_{m,\lambda}(\mathbf{k}) \quad (2.9)$$

where  $\varphi_{im}(\mathbf{r})$  is the localised orbital with quantum number  $m$  on site  $i$ . Coefficients  $A_{ij}$  satisfy the equation  $\mathbf{H}\mathbf{A} = \mathbf{S}\mathbf{A}\mathbf{E}$  with the normalisation  $\mathbf{A}^\dagger\mathbf{S}\mathbf{A} = 1$ . Here  $\mathbf{E}$  is the diagonal matrix of eigenvalues  $\epsilon(\mathbf{k}, \lambda)$ , and  $\mathbf{H}$  and  $\mathbf{S}$  are the Fourier-transformed tight-binding Hamiltonian and overlap matrices respectively. Equation (2.1) is re-cast in the form

$$\omega(\mathbf{q}_j)^2 = D_0 + D_1 + D_2 \quad (2.10)$$

where  $D_0$  represents the contribution to the dynamical matrix from direct nucleus–

nucleus interactions less than from the self-energy of the electrons.  $D_1 + D_2$  represent contributions from the one-electron band-structure energy

$$E_{\Sigma} = \sum_{\mathbf{k}, \lambda} \varepsilon(\mathbf{k}, \lambda) f(\mathbf{k}, \lambda)$$

and may be written in terms of the variations in  $H_{in,jm}$  and  $S_{in,jm}$  as the atoms are moved. In elemental crystals  $D_0 + D_1$  contain only short-range forces and hence are unlikely to give rise to softening phonon modes. Whether this still remains the case in the layered TMDs where there is more than one atom per unit cell has not been investigated much as yet. The remaining contribution,  $D_{\alpha\beta}^{(2)}(\mathbf{q})$ , which Varma and Weber have found to be responsible for the observed phonon anomalies in all the metallic transition-metal compounds they investigated, is given by

$$D_{\alpha\beta}^{(2)}(\mathbf{q}) = \sum_{\mathbf{k}, \lambda, \lambda'} g^{\alpha}(\mathbf{k}, \lambda; \mathbf{k} + \mathbf{q}, \lambda') * g^{\beta}(\mathbf{k} + \mathbf{q}, \lambda'; \mathbf{k}, \lambda) \frac{f(\mathbf{k}, \lambda) - f(\mathbf{k} + \mathbf{q}, \lambda')}{\varepsilon(\mathbf{k}, \lambda) - \varepsilon(\mathbf{k} + \mathbf{q}, \lambda')} \quad (2.11)$$

Here, the fully self-consistent electron-phonon matrix element  $g^{\alpha}(\mathbf{k}\lambda; \mathbf{k} + \mathbf{q}\lambda')$  describes the scattering of an electron from a Bloch state  $(\mathbf{k}, \lambda)$  to a Bloch state  $(\mathbf{k} + \mathbf{q}, \lambda')$  as the ions are moved in the  $\alpha$ th cartesian direction, and is given by

$$g^{\alpha}(\mathbf{k}, \lambda; \mathbf{k} + \mathbf{q}, \lambda') = \sum_{m,n} A_{\mu m}^*(\mathbf{k}) [(\gamma_{mn}^{\alpha}(\mathbf{k}) - \gamma_{mn}^{\alpha}(\mathbf{k} + \mathbf{q})) - \varepsilon(\mathbf{k}, \lambda)(\sigma_{mn}^{\alpha}(\mathbf{k}) - \sigma_{mn}^{\alpha}(\mathbf{k} + \mathbf{q}))] A_{n\mu'}(\mathbf{k} + \mathbf{q}) \quad (2.12)$$

where

$$\gamma_{mn}^{\alpha}(\mathbf{k}) - \varepsilon(\mathbf{k}, \lambda)\sigma_{mn}^{\alpha}(\mathbf{k}) = \sum_{R_{ij}} |\nabla_{\alpha} H_{im,jm} - \nabla_{\alpha} S_{im,jn}| \exp i\mathbf{k} \cdot \mathbf{R}_{ij} \quad (2.13)$$

To obtain the Hamiltonian and overlap matrices needed in the above formulation would require, in general, a complete tight-binding fit to the full band structure, which in turn would require a basis set of atomic orbitals on each atom in (2.9) from 1s up. In practice a fitting scheme using a much reduced basis set (five metal d orbitals and three chalcogen p orbitals in the case of Doran *et al* 1978a,b) is used to fit to the valence and conduction bands in the layered TMDs. The distance dependencies of the Hamiltonian and overlap matrices needed for the determination of the matrix elements are determined by refitting to the band structure of a structure compressed or expanded by  $\approx 5\%$ .

Varma and Weber (1979) ultimately gain also an approximate expression for the above matrix elements in terms of the difference of the electron velocities of the states

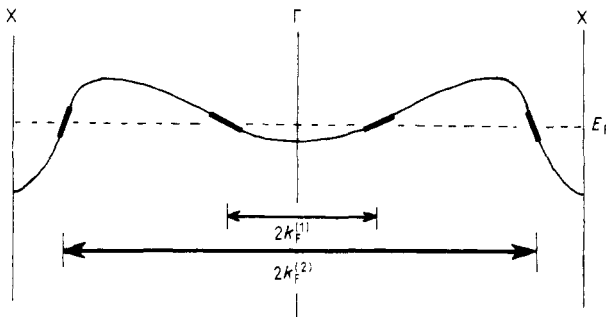


Figure 2. Nesting instability  $2k_F^{(2)}$  would be preferred over  $2k_F^{(1)}$  (where  $v_F$  is small) in this simple one-dimensional band. Density-of-states effects may reverse this in three dimensions.

$(\mathbf{k}, \lambda)$  and  $(\mathbf{k} + \mathbf{q}, \lambda')$ :

$$g^\alpha(\mathbf{k}, \lambda; \mathbf{k} + \mathbf{q}, \lambda') \sim (v^\alpha(\mathbf{k}, \lambda) - v^\alpha(\mathbf{k} + \mathbf{q}, \lambda')) \sum_m A_{\mu m}^*(\mathbf{k}) A_{\mu' m}(\mathbf{k}) \quad (2.14)$$

where  $v^\alpha(\mathbf{k}, \lambda) = \partial \varepsilon(\mathbf{k}\lambda) / \partial k^\alpha$ . Thus the matrix elements  $g^\alpha$  are large when they couple states with large and opposite band dispersion along the  $\alpha$ th component of wave-vectors  $\mathbf{k}$  and  $\mathbf{k} + \mathbf{q}$  (figure 2). The CDW/PLD state is encouraged as lattice distortions at certain wave-vectors cause a relatively large modification in the electronic energy.

The untangling, indeed the relevance, of the above factors to the condensation of CDW/PLD states in real systems as diverse as the layered TMDs, the organic charge-transfer salts,  $\alpha$ -uranium, (?), potassium (?) . . . , to which many of the supposed archetypal features such as perfect nesting, uniform gapping of a simple band structure, applicability of a harmonic analysis and weak coupling may no longer apply, is a massive task. In what follows we will tend to concentrate on the CDW/PLD instabilities observed in the layered TMDs both because this is where our major interests lie, and also since we believe it to be essential to base discussion on a real class of compounds. We begin then with a brief summary of the structural and electronic characteristics of the layered TMDs.

### 3. Structural and electronic characteristics of the layered TMDs

The TMDs of the group IVB, VB and VIB transition metals form layer compounds in which a sheet of metal atoms is sandwiched between sheets of chalcogens, with only relatively weak forces between successive  $\text{TX}_2$  sandwiches. Each metal atom is coordinated by six chalcogens in either an octahedral (1T) or trigonal prismatic (2H) arrangement of covalent bonds (see figure 3). The electronic structure consists of broad bonding

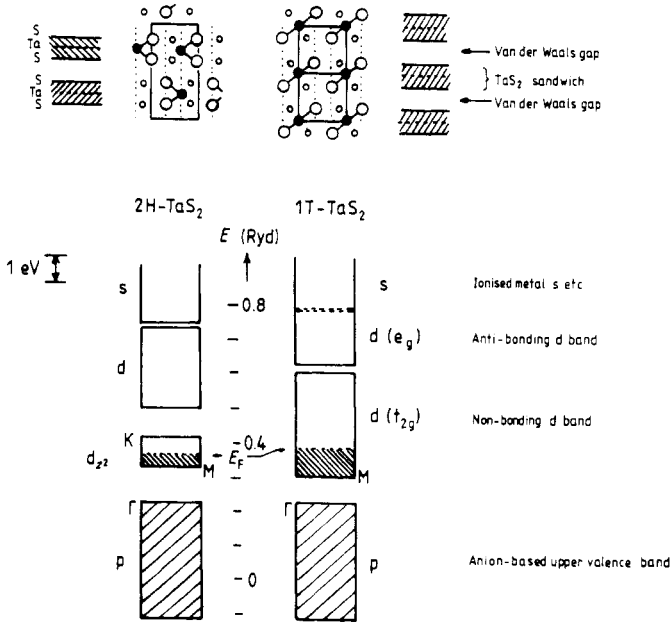


**Figure 3.** The crystal structures and band structures for 2H- and 1T-TaS<sub>2</sub>, which respectively display trigonal prismatic and octahedral coordination of Ta atoms. The block band structures are based on the APW results of Mattheiss (1973).

and anti-bonding bands formed from the metal and chalcogen orbitals, with non-bonding bands formed from certain of the metal d orbitals sitting in between (Wilson and Yoffe 1969, Inglesfield 1980). Each chalcogen has six s/p electrons available for bonding to neighbouring metal atoms and each metal atom is required to contribute four electrons to fill the bonding bands (16e). The group IVB elements can just do so. The extra electron in the group VB compounds (V, Nb, Ta) then enters the non-bonding d bands, the result being moderately good but rather two-dimensional metals, with typical conductivity anisotropies of  $\approx 30$  (Edwards and Frindt 1971).

Band-structure calculations for most of the 1T and 2H materials have been made using a variety of different methods (see Bullett 1978). Figure 4 shows the band structure of (pre-CDW) 1T-TaS<sub>2</sub> as calculated by the layer method (Woolley and Wexler 1977). A typical ratio of the conduction band width within the layer to that perpendicular to the layer is five. Thus the group VB layered TMDs are far from being extremely two-dimensional electronically. The overall  $t_{2g}$  conduction band width for 1T-TaS<sub>2</sub> and 1T-TaSe<sub>2</sub> is  $\approx 2.7$  eV, while that for the  $d_{z^2}$  band of the 2H polytypes is  $\approx 1.3$  eV. Thus one might expect stronger electron-phonon matrix elements for these 1T polytypes. Figure 5 shows the basal-plane resistivity of 1T- and 2H-TaS<sub>2</sub> along with similar plots for the selenides. Apart from the obvious existence of phase transitions a striking feature of

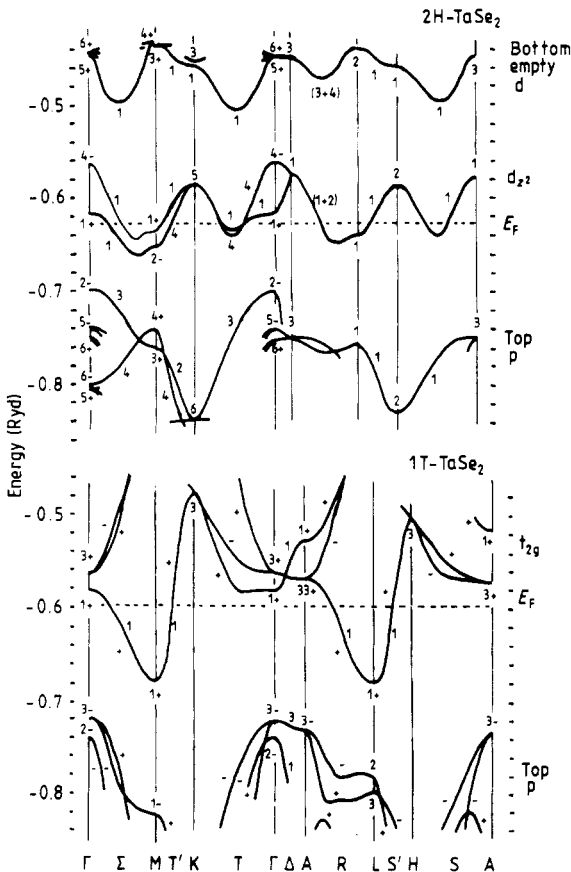


**Figure 4.** Band structures of 1T- and 2H-TaSe<sub>2</sub> in the vicinity of  $E_F$  as determined by the layer method (Woolley and Wexler (1977), Doran *et al* (1978b), respectively).

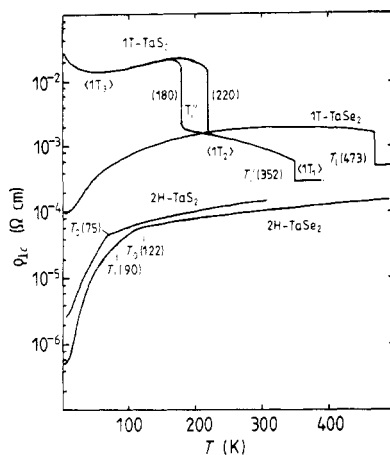


**Figure 5.** The contrasting resistivity behaviour of 2H- and 1T-TaS<sub>2</sub> and 1T-TaSe<sub>2</sub> (DiSalvo 1977). Note the divergence between 1T-TaS<sub>2</sub> and TaSe<sub>2</sub> at low temperatures due to structural complexities of the former (see later) and the carrier localisation so induced. For each  $\rho \approx (2-5) \times 10^{-4} \Omega \text{ cm}$  by 500 K. Metastable 1T polytypes rapidly revert to trigonal prismatic types above this temperature, i.e. prior to reaching their CDW onset,  $T_0$ .

figure 5 is the large values of the high-temperature resistivities. Such large values of resistivity correspond to very short scattering times for the conduction electrons ( $\tau \approx 2.3 \times 10^{-15} \text{ s}$  for  $\rho = 1 \times 10^{-4} \Omega \text{ cm}$ ) with mean free paths of the order of 20 Å and Dingle temperatures  $h/\tau \approx 0.2-0.3 \text{ eV}$  (Friedel 1985). Blurring of the Fermi surface due to temperature-dependent effects is thus swamped by blurring due to incoherent electron-phonon scattering for temperatures  $< 1000 \text{ K}$  (Huntley *et al* 1978).

The vibrational properties of the various polytypes are strongly influenced by the properties of the metal-chalcogen bond (Schmid 1976). The three-dimensional structure of a sandwich affects considerably the character of the intra-layer vibrational modes. In particular, the longitudinal acoustic (LA) branches (whose frequency tending to zero signals the incipient CDW/PLD instability; see Moncton *et al* (1977), Ziebeck *et al* (1977); see also Moncton (1975) have lowish frequencies, as opposed to those in a truly two-dimensional layered material such as graphite, because of the mixed  $x$  and  $z$  character of the displacements which combine in such a way as to preserve the metal-chalcogen bond length. In the case of group IVB dichalcogenides like HfS<sub>2</sub>, the observed dispersion of the LA branches is essentially determined by such metal-chalcogen bond-bending interactions (Wakabayashi *et al* 1975, Feldman 1982).

The CDW/PLD instabilities endemic to the group VB dichalcogenides (Wilson *et al* (1975); see also Wilson *et al* (1974)), with their one extra electron and their characteristic softening of the LA phonon mode, are in very general terms the consequence of attractive metal-metal interactions (Feldman 1982, Haas 1978, 1979) from overlap of the non-bonding metal-atom d orbitals (Doran *et al* 1978a,b).

As a function of temperature there occurs a whole series of phase transitions within the group V layer TMDs involving a remarkable variety of CDW/PLD phases (Wilson *et al* 1975, Moncton *et al* 1977, McWhan *et al* 1980, Fung *et al* 1981, Tsutsumi 1982). Typically the sequence on cooling is from a high-temperature 'undistorted' phase, characterised by the absence of sharp superlattice spots in diffraction patterns, through an intermediate 'nearly commensurate' incommensurate phase (or phases), to a low-temperature commensurate CDW/PLD superstructure. On warming from the com-

mensurate phase there sometimes is a transition into a further state characterised by a breaking of the usual threefold symmetry with respect to CDW/PLD wave-vector positions. The high-temperature  $1T_1$  CDW phases of  $TaS_2$  and  $TaSe_2$  (see Wilson *et al* (1975), figure 13) together with the triple- $q$  phase of  $1T-VSe_2$  (Eaglesham *et al* 1986) are characterised by the coexistence of sharp CDW/PLD satellites along with a complicated pattern of diffuse intensity. Moreover the diffraction patterns of the 'undistorted' phase of the  $2H$  polytypes also contain a diffuse intensity distribution (Chevalier and Stobbs (1975); Wilson *et al* (1975), figure 7). Some authors have attributed the latter scattering to a CDW/PLD distortion exhibiting short-range order only.

The production of these various condensed states within the electronic/lattice structure may be detected by diverse techniques such as x-ray photo-emission (Hughes and Pollak 1976), Mossbauer spectroscopy (Pfeiffer *et al* 1984, Eibschutz 1986), TDPAC, (Butz *et al* 1979, 1986), NMR (Pfeiffer *et al* 1982, Naito *et al* 1985a,b), angle-resolved photo-emission spectroscopy (ARPES) (Smith *et al* 1985) and scanning tunnelling (Slough *et al* 1986).

Theoretical efforts to understand and correlate the large range of experimental observations made upon the group V layered TMDs have generally taken one of two approaches. The first approach involves Landau-like free-energy expansions, first introduced for these compounds by McMillan (1975). This approach has been very successful in explaining many observations, from the original prediction that discommensurate states should exist (McMillan 1976) to more recent work incorporating the observed orthorhombic symmetry in  $2H-TaSe_2$  (Walker and Jacobs 1982, Littlewood and Rice 1982, Nakanishi and Shiba 1983, Shiba and Nakanishi 1986). It is not, however, a true microscopic approach and cannot predict transition temperatures, CDW/PLD instability wave-vectors, or, indeed, whether the transitions should occur at all. Consequently, we now turn our attention to alternative microscopic theoretical calculation. We shall return to discuss the characteristics of the various CDW/PLD states mentioned above in later sections. We shall return also to questions concerning the use of Landau theory.

#### 4. Assessing relative roles played in CDW/PLD formation, with particular reference to the layer TMDs

##### 4.1. The role of $\chi^0(\mathbf{q})$

A function clearly of considerable importance in encouraging CDW/PLD instabilities is the non-interacting electronic susceptibility  $\chi^0(\mathbf{q})$  as given in (2.7). Large  $\chi^0(\mathbf{q})$  implies a large gain to be made in one-electron band-structure energy, while any strong wave-vector dependence singles out the likely wave-vector for the incipient instability. Clearly the individual contributions to such an expression are maximised when the energy denominator in (1.6) is small (i.e. for scattering of the conduction electrons from one side of the Fermi surface to the other). Any overall peaking in  $\chi^0(\mathbf{q})$  as a function of wave-vector must arise from regions of  $\mathbf{k}$ -space close to the Fermi surface, and the many such  $q$ -coupled electron states needed in this demands a high overall density of states in the close vicinity of the Fermi surface—hence any large radius of curvature to the surface is a feature of potential importance.

A three-dimensional free-electron Fermi surface gives rise only to a weak gradient singularity with no peak in  $\chi^0(\mathbf{q})$ . As the dimensionality is reduced, however, the

singularities and peaks in  $\chi^0(\mathbf{q})$  develop. A square-root singularity occurs for the case of a two-dimensional Fermi cylinder, while a divergent logarithmic instability ( $\chi^0(\mathbf{q} = 2k_F) \sim \frac{1}{2}N(E_F) \ln(E_F/kT)$ ; Rice and Strässler 1973) occurs for the case of a perfectly nested one-dimensional Fermi surface. For cases between a planar and cylindrical FS, as shown by Fehner and Loly (1974), a finite peak in  $\chi^0(\mathbf{q})$  occurs, the form and position of which is largely a function of the size and radii of curvature of the regions of the Fermi Surface being nested. Significant nesting can also be obtained from saddle points (Rice and Scott 1975, Wilson 1977).

In the case of the quasi-one-dimensional metals, such as KCP and TTF-TCNQ, the distorted structure has a wave-vector component along the chain direction exactly in line with the particular 1D band-filling (Renker and Comès 1975). This very strongly defined intra-chain  $q$ -dependence arising from  $\chi^0(\mathbf{q})$  is made apparent in the sharp one-dimensional Kohn anomalies observed above onset in the softening LA mode at  $q = 2k_F$ . In the case of the quasi-two-dimensional TMDs, however, the role assignable to  $\chi^0(\mathbf{q})$  is much diminished. Myron *et al* (1977), for example, have calculated the conduction band contribution to  $\chi^0(\mathbf{q})$  for 1T-TaS<sub>2</sub> and 1T-TaSe<sub>2</sub> from their KKR band-structure results. Although they do find a peaking in  $\chi^0(\mathbf{q})$  close to the observed CDW wave-vector positions, it is noteworthy that the calculated peaking is not great, certainly not divergent, and that  $\chi^0(\mathbf{q})$  is substantial over large regions of the Brillouin zone (see figure 6). Similarly Doran

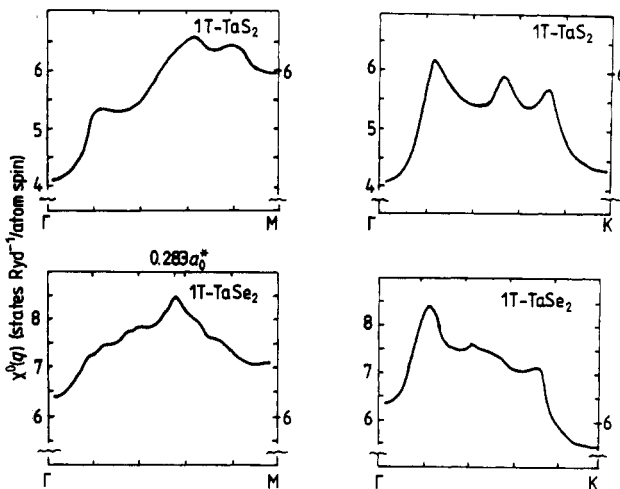


**Figure 6.**  $\chi^0(\mathbf{q})$  for 1T-TaSe<sub>2</sub> and 1T-TaS<sub>2</sub> on  $\Gamma M$  and  $\Gamma K$  axes. The maximum on  $\Gamma M$  is very close to the observed  $q^{(CDW)}$ . (Based on Myron *et al* 1977.) Note the different scales and offset origin.

*et al* (1978b) have found  $\chi^0(\mathbf{q})$  for the 2H polytypes to take a broadly humped form, being high over most of the outer portions of the Brillouin zone. This much weaker  $q$ -dependence of  $\chi^0(\mathbf{q})$  is made evident in the much broader two-dimensional Kohn anomalies that are observed above onset in these quasi-two-dimensional systems (Moncton *et al* 1977).

A consequence of inter-chain/inter-layer hopping in low-dimensional metals is to 'buckle' the quasi-one-/two-dimensional Fermi surfaces. Such an expansion in dimensionality allows for a development of long-range order in the transverse direction also, and so may lead to a three-dimensional character to events. The effect that this has upon the onset transition temperatures and wave-vector dependences of CDW/PLD instabilities

has been considered in some detail for the quasi-one-dimensional compounds (Horowitz *et al* 1975, Friend and Jérôme 1979, Friedel 1985), but has not been much considered as yet for the layered TMDs.

In the case of the 1T polytypes Myron *et al* (1977) considered the effect of the band structure normal to the layers to be of little importance, whereas Woolley and Wexler (1977) have predicted that  $\chi^0(\mathbf{q})$  should depend strongly upon the wave-vector component  $q_z$  perpendicular to the layers. The existence in 1T-VSe<sub>2</sub> of sharp CDW/PLD satellite spots below  $\approx 110$  K which are incommensurate perpendicular to the layers ( $\approx 0.31c^*$ ) while being apparently commensurate within the layers ( $0.25a^*$ ) is further evidence for the importance of the band structure normal to the layers in these materials (Tsutsumi 1982).

The case of the 2H polytypes is somewhat complicated by the presence of a double-sheeted Fermi surface due to the two formula units per unit cell. The calculation by Doran *et al* (1978b) of the conduction electron contribution to  $\chi^0(\mathbf{q})$  was made under the assumption of no inter-sheet scattering. The marked  $c^*$  axis variation in the Fermi surface means, then, that such a calculation leads to different contributions to  $\chi^0(\mathbf{q})$  from different heights  $k_z c^*$  in the Brillouin zone (see figure 3 of Doran *et al* 1978b). If inter-sheet scattering within the conduction band is allowed, it is qualitatively clear that one can obtain a much more 'two-dimensional'  $\chi^0(\mathbf{q})$  showing more peaked structure.

Such considerations help in understanding both the nature and strength of the inter-layer interactions in the 2H polytypes (Bird and Withers 1985), in addition to the precise wave-vector adopted by the observed CDW/PLD instabilities. With further regard to the wave-vector dependence, the results of Motizuki and Ando (1983), obtained from a fit to the Mattheiss (1973) band structure, demonstrate the high sensitivity that any peaking in  $\chi^0(\mathbf{q})$  has to the details of the Fermi surface states.

The temperature dependences of  $\chi^0(\mathbf{q})$  in quasi-one- and two-dimensional CDW/PLD systems differ qualitatively. The intimate nesting involved in the one-dimensional case leads to a  $\chi^0(\mathbf{q})$  peak that is very sensitive to temperature-dependent smearing of the Fermi surface. On the other hand calculations of the temperature dependence of the  $\chi^0(\mathbf{q})$  hump for the layered TMDs tend to find a decrease of only 10% as the temperature is increased from  $T = 0$  K to several hundred kelvin (Doran *et al* 1978a,b).

In conclusion the weak, clearly non-divergent wave-vector dependences of  $\chi^0(\mathbf{q})$  for two-dimensional CDW/PLD systems suggest that  $\chi^0$  is not the major factor to determine whether—or even at what wave-vector—a CDW/PLD instability is going to occur. Clearly the electron–phonon and electron–electron interactions are playing essential roles in establishing the observed behaviour of these 2D systems.

#### 4.2. The role of the matrix elements $g^\alpha(\mathbf{k}, \lambda; \mathbf{k} + \mathbf{q}, \lambda')$ in CDW/PLD formation

Large matrix elements  $g^\alpha(\mathbf{k}, \lambda; \mathbf{k} + \mathbf{q}, \lambda')$  require steep bands along the  $\alpha$ th component of the wave-vectors  $\mathbf{k}$  and  $\mathbf{k} + \mathbf{q}$  (see (2.15)). On the other hand  $\chi^0(\mathbf{q})$  is maximised for flat bands. Clearly there is some sort of competition going on that determines the relative influence of  $\chi^0(\mathbf{q})$  and  $g^\alpha(\mathbf{k}, \lambda; \mathbf{k} + \mathbf{q}, \lambda')$  upon the one-electron band-structure contribution to the dynamical matrix  $\mathbf{D}_2(\mathbf{q})$  (see (2.12)). In Varma and Weber (1979) and Weber (1980), the authors were able to show in the case of Nb–Mo alloys that the wave-vector dependence of the various observed phonon anomalies were determined there by the wave-vector dependence of the matrix elements  $g^\alpha$ , with no strong nesting tendency dominating the wave-vector dependence of  $\chi^0(\mathbf{q})$ . It is necessary accordingly to consider the magnitude, the wave-vector dependence, and the PLD eigenvector dependence of

the matrix elements  $g^\alpha(\mathbf{k}, \lambda; \mathbf{k} + \mathbf{q}, \lambda')$  for our CDW/PLD reference compounds, the layer TMDs.

The most detailed, self-consistent results have been obtained by Doran and Woolley (1981, 1983) via a tight-binding fit to the valence and conduction bands of 2H-NbSe<sub>2</sub> obtained earlier by the layer method. They found that the Hamiltonian and overlap parameters fitted well to an  $R^{-n}$  behaviour ( $R$  = inter-atomic distance). For the metal-metal (dd) parameters  $n$  was very close to five, whereas the metal-ligand (dp, ds) parameters were found to be far less sensitive to distance changes and behaved as  $R^{-2}$ . As the gradients of  $H$  and  $S$  required for the calculation of  $g^\alpha$  (in (2.12) and (2.13)) are proportional to  $n$ , and as the overall energy lowering  $\mathbf{D}_2$  is proportional to  $n^2$ , it is clear that the conduction electrons are much more strongly affected by changes in the metal-metal inter-atomic distances than by changes in the metal-chalcogen or chalcogen-chalcogen distances. The strength of the d-electron electron-phonon coupling in these materials is evident in the large values of the high-temperature resistivities, as mentioned in § 3.

Inglesfield (1980) has in essence calculated  $\mathbf{D}_2$  as a function of wave-vector for longitudinal phonons in the case of 1T-TaS<sub>2</sub>. He found a large singularity along the  $\Gamma\text{M}$  direction at  $\mathbf{q} = 0.65\Gamma\text{M}$  which he attributes to the effect of nesting rather than to a 'much less rapid' variation of matrix elements with wave-vector. However, the only really quantitative calculation of the wave-vector and PLD eigenvector dependences of  $g^\alpha(\mathbf{k}, \lambda; \mathbf{k} + \mathbf{q}, \lambda')$  for the group VB layered TMDs comes from the work of Motizuki and colleagues (Yoshida and Motizuki 1982, Motizuki and Ando 1983). Motizuki and Ando have calculated the conduction band contributions to  $g^\alpha(\mathbf{k}, \lambda; \mathbf{k} + \mathbf{q}, \lambda')$  as a function of  $\mathbf{k}$  for three different  $\mathbf{q}$ -vectors ( $\mathbf{q} = \frac{2}{3}\Gamma\text{M}$ ,  $\Gamma\text{M}$  and  $\frac{1}{2}\Gamma\text{K}$ ) in the case of 2H-TaSe<sub>2</sub> and 2H-NbSe<sub>2</sub>.  $g^\alpha$  was found to depend quite strongly upon the wave-vector  $\mathbf{k}$ . For each of the three  $\mathbf{q}$ -vectors selected, a large value of  $g^\alpha$  occurred when  $\mathbf{k}$  and  $\mathbf{k} + \mathbf{q}$  were both close to the Fermi surface. The maximum value of  $g^\alpha$  for  $\mathbf{q} = \frac{2}{3}\Gamma\text{M}$  was almost the same as for  $\mathbf{q} = \frac{1}{2}\Gamma\text{K}$  but only a little over half that for  $\mathbf{q} = \Gamma\text{M}$ . Their final calculated  $\mathbf{D}_2(\mathbf{q})$  indicate nonetheless that the wave-vector dependence of  $g^\alpha$  has not become dominant. The calculations did show a strong dependence upon the polarisation of the metal-atom vibrations, with longitudinal distortions very strongly favoured. Surprisingly in the case of 1T-VSe<sub>2</sub> (Yoshida and Motizuki 1982) transverse displacements of the metal atoms within the basal plane were calculated to be almost as favourable as longitudinal distortions.

As in the last section, then, the major lesson is that there is no one overwhelmingly dominant factor governing CDW/PLDs in 'two-dimensional' systems, be it either  $\chi^0(\mathbf{q})$  or  $g^\alpha(\mathbf{k}, \lambda; \mathbf{k} + \mathbf{q}, \lambda')$  or  $\omega^B(\mathbf{q})$ , and consequently there can be no substitute for detailed microscopic calculations to present the situation adequately.

#### 4.3. Band-structure energy lowering and CDW/PLD superstructures

Doran and Woolley (1981), as well as others like Campagnoli *et al* (1980) and Smith *et al* (1985), have calculated the band structure near the 2H Fermi energy in the presence of a 3a commensurate CDW/PLD superlattice. Although the calculations generally include only changes in the metal-metal hopping parameters, there is one very important general conclusion immediately to be drawn. This is that the CDW/PLD does not open one uniform gap at the Fermi energy, but rather, this being a many-band situation, band degeneracies are lifted and bands become shifted over most of the Brillouin zone (see figure 7). In the case of the 2H polytypes Doran and Woolley (1981) indicate that there will be a whole

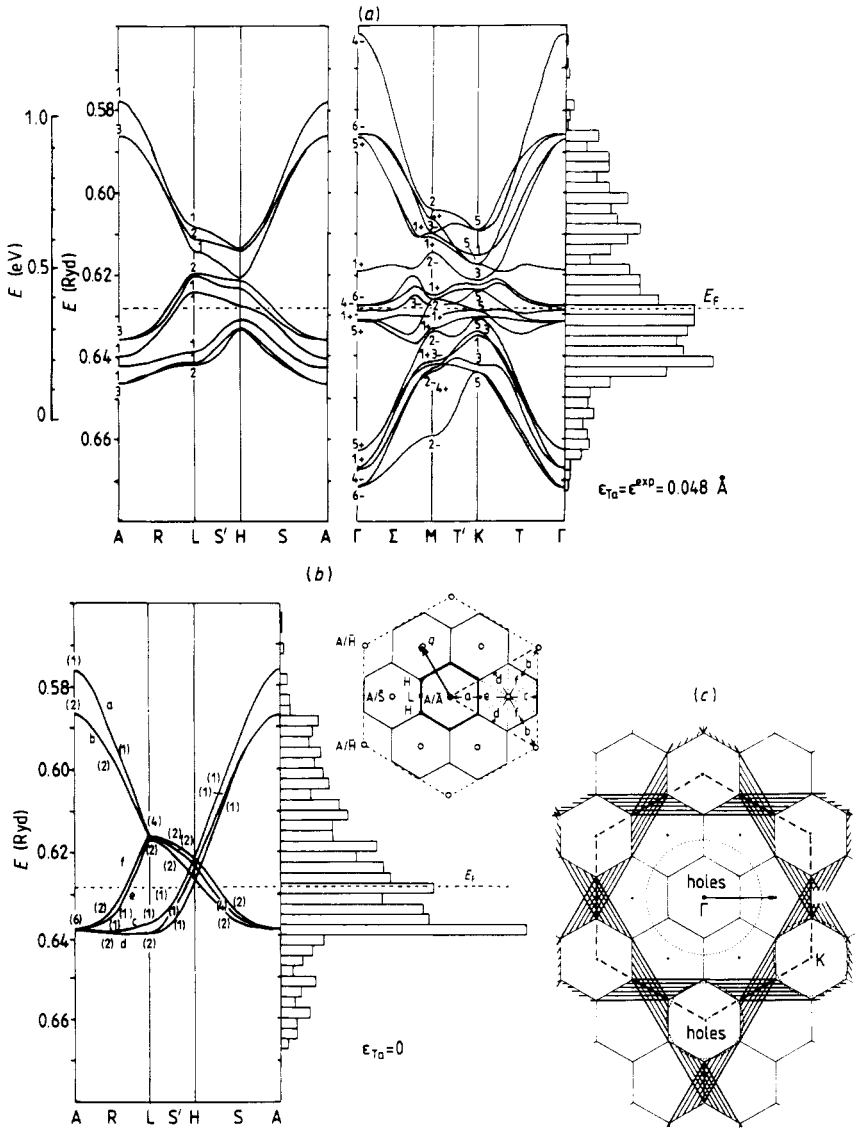


**Figure 7.** The 2H  $d_{z^2}$  band for 2H-NbSe<sub>2</sub> as reformed in the presence of an  $\alpha\alpha 3^{\oplus}$  type- $3a_0$  CCDW (of magnitude, as well as phasing, as originally suggested from the neutron work of Moncton *et al* 1977). The calculations were made by Doran and Woolley (1981), comparison being made to a zero-potential band-folding in order to illustrate the multi-sited gapping. Part (c) shows the triple-axis nesting involved (see Wilson 1977). In (a) bracketed numbers on bands are degeneracies and small letters refer to parentage of band in original zone (see inset). FS shown dotted.

range of new optical transitions induced by the CDW/PLD, many of which will occur in the vicinity of 0.35 eV almost irrespective of the amplitude of the CDW/PLD. Experimentally, Campagnoli *et al* (1980) do observe a whole series of new optical transitions occurring between 0.3 to 0.8 eV following onset of the CDW/PLD in 2H-TaSe<sub>2</sub>. Clearly such transitions do *not* provide any measure of the band-structure energy lowering due to the CDW/PLD, contrary to what is often claimed.

By summing over the occupied condition band states Doran and Woolley (1981) found that the electronic energy gain due to the commensurate triple- $q$  CDW/PLD superlattice of 2H-TaSe<sub>2</sub> was approximately quadratic in the CDW/PLD amplitude. For a PLD amplitude of 0.048 Å (as is recently affirmed by Bird *et al* (1985) for 2H-TaSe<sub>2</sub> at 60 K) this energy gain was 26 meV/Ta atom (see figure 8). In the case of 1T-TaS<sub>2</sub> Smith *et al* (1985) find a very much stronger change in the Ta d conduction band, which of course simply reflects the much greater amplitude of the CDW/PLD in this case (Brouwer and Jellinek 1980). Unfortunately there was no comparable calculation of the band-structure energy lowering.

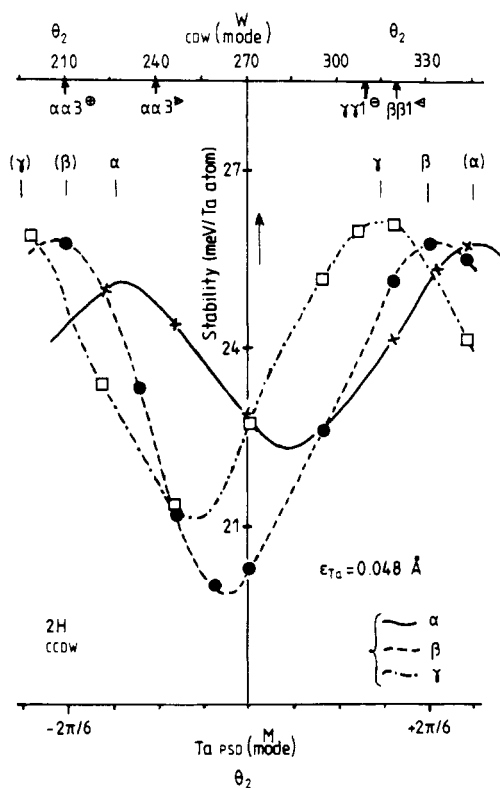


**Figure 8.** The oscillations in stability for  $\alpha$ -,  $\beta$ - and  $\gamma$ -type  $3a_0$  CCDWs with change in the internal phase angle ( $\theta_2$  is used) relative to their point of common phasing (given both for Ta PSD in the Moncton mode of definition, and for the associated CDW in the Wilson mode of definition; see Doran and Woolley 1981, 1983, Wilson 1985b). Note that the stabilisation wrought here by any phasing choice change (and hence by lock-in) is very slight.

A further important feature clearly apparent in Doran and Woolley's work on the 2H polytypes is that the bulk of the above electronic energy gain is independent of the detailed phasing of the CDW/PLD. For the case where each of the three CDW/PLDs was given like phasing and an identical PLD amplitude of 0.096 Å, the electronic energy gain as a function of the common phase angle was found to oscillate only by  $\pm 5$  meV about a mean stabilisation of  $-93$  meV/Ta atom. Thus the majority of the electronic energy gain is quite independent of the detailed atomic displacement pattern, or indeed of whether by implication the CDW/PLD wave-vectors are commensurate or incommensurate. To date there has been no analogous calculation for any of the 1T polytypes.

It certainly would be interesting to find the influence of the phase-dependent 'bonding' terms for, say, 1T-TaS<sub>2</sub>. It might be thought that the relative influence of specific bonding terms in 1T-TaS<sub>2</sub> should be more substantial than in the 2H polytypes due to the larger change in the heat of enthalpy that is found at the incommensurate–commensurate lock-in transition in the case of the 1T polytype. On the other hand, it could be argued that this is simply due to a larger change in CDW/PLD amplitudes at the lock-in transition in 1T-TaS<sub>2</sub> and says nothing about the relative influence of phase-dependent bonding interactions.

In light of the discovery by Fung *et al* (1981) that the CDW/PLD superlattice in 2H-TaSe<sub>2</sub> had orthorhombic and not hexagonal symmetry, Doran and Woolley (1983) subsequently proceeded to calculate the electronic energy gain as a function of phase angle for the three limiting types of superlattice considered in the theoretical work of McMillan (1982) and Walker and Jacobs (1982). The results are included in figure 8, where the maxima correspond to the most favourable situations. The very small differences in energy between the maxima of the three curves imply that microscopic calculations, at the present level of sophistication, are simply incapable of predicting the detailed atomic displacement patterns of CDW/PLD superstructures. In particular, the approximation of including only changes in the metal–metal hopping parameters, and ignoring changes in the phase-dependent interlayer hopping parameters, is clearly unreasonable if one is hoping accurately to determine the phase dependence of the band-structure energy lowering, let alone predict the detailed atomic displacement patterns. One significant improvement that is needed is undertaking all the band-structure work relativistically: TaSe<sub>2</sub> is a very heavy material. This could also provide a suitable introduction to the magnetic behaviour of these materials (see Wilson and Vincent 1984, Wilson 1985b, Butz *et al* 1986).

#### 4.4 Should a CDW/PLD instability occur at all?

The question as to whether CDW/PLD instabilities are ever going to arise on cooling, and if so in what wave-vector range, involves the balancing of short-range and electronic contributions. The electronic contribution as shown in § 4.2 is dominated by changes in the metal–metal separation distances. This point has been recast by some authors (Haas 1978, Inglesfield 1980) as a general tendency to form metal–metal d bonds, and widely used to justify considering only changes in metal–metal parameters when the electronic contributions to the dynamical matrix  $\mathbf{D}_2(\mathbf{q})$  are calculated (Doran and Woolley 1981, Inglesfield 1980, Feldman 1982). Clearly such calculations can then say little about the relative motion of the metals and chalcogens. The behaviour of any softening phonon mode, however, depends too upon the short-range contributions to the dynamical matrix represented by  $\mathbf{D}_0 + \mathbf{D}_1$  in (2.11).

Feldman (1982) has given a phenomenological lattice dynamical model for the 2H polytypes. This involves deriving the softening of the two anomalous  $\Sigma_1$  LA phonon modes (Moncton *et al* 1977) by means of a strongly wave-vector-dependent metal–metal interaction. The short-range portion of the dynamical matrix was parametrised in terms of valence force-field parameters, and the strongest of these clearly 'tries' to keep the metal–chalcogen bond lengths constant in the face of changing metal–metal inter-atomic separations. In terms of the electronic structure it is clear that any change in the metal–chalcogen bond lengths must strongly affect the chalcogen p-based valence bands, and act thereby to restrain the advance of the structural instability. The ability to shift the non-metal atoms at relatively little energy cost into the soft van der Waals regions of

one- and two-dimensional structures is a major factor in the facility of these materials for bearing CDW/PLDs. Direct illustration of this is gained in the lithium-intercalated IVB materials like  $\text{Li}_x\text{ZrSe}_2$  which, although basically iso-structural (apart from the Li) and iso-electronic with 1T-TaSe<sub>2</sub> or VSe<sub>2</sub>, develop very weak CDWs (Klipstein *et al* 1984).

The most detailed study of the lattice instability and lattice dynamics in a group VB layered TMD is the work of Motizuki *et al* (1984) on 2H-TaSe<sub>2</sub> and 2H-NbSe<sub>2</sub>. This paper suggests that harmonic instability at  $T = 0$  K is limited to a narrow range of wave-vectors for both materials, and implies that the observed onset transition temperatures can be understood from a purely harmonic analysis. They do, however, note that their calculated  $\Sigma_1$  phonon frequencies are very sensitive to the value of  $\mathbf{D}_2(\mathbf{q})$ . An increase in  $\mathbf{D}_2$  of about 10% results in harmonic instability even at 500 K. Since the derivatives of the Hamiltonian and overlap integrals needed to calculate the electron-phonon matrix elements  $g^\alpha$  were estimated, rather than self-consistently calculated, there is clearly scope for error in their calculation of  $\mathbf{D}_2(\mathbf{q})$ . What is more, the calculations yield a huge temperature-dependent splitting ( $\approx 10$  meV at 300 K) between the two  $\Sigma_1$  longitudinal acoustic modes, which in the absence of inter-layer interactions would be degenerate (Feldman 1982). The experimental dispersion curves of Moncton *et al* (1977) are clearly inconsistent with this large splitting.

Using simplified band-structure models for 2H- and 1T-TaS<sub>2</sub>, Inglesfield (1980) had earlier calculated a maximum  $\mathbf{D}_2(\mathbf{q})$  at 65 K of  $-6.8 \text{ eV \AA}^{-2}$  and  $-7.7 \text{ eV \AA}^{-2}$  respectively. The opposing short-range contribution to the dynamical matrix (for both materials) was estimated by extrapolation of the LA room-temperature phonon dispersion curve of 1T-TaS<sub>2</sub> (Ziebeck *et al* 1977) to obtain an estimated LA phonon mode frequency in the absence of electronic effects. To convert this estimated frequency (2.9 THz) into a force constant requires squaring the frequency and multiplying by a mass. Inglesfield used an average mass  $\bar{m} = \frac{1}{3}(m_{\text{Ta}} + 2m_{\text{S}})$ , and so estimates the opposing short-range contribution for both 2H- and 1T-TaS<sub>2</sub> to be  $\approx 2.9 \text{ eV \AA}^{-2}$ . Accordingly the conclusion he reached is that at  $T = 0$  K harmonic instability should occur for a large range of wave-vectors in both 2H- and 1T-TaS<sub>2</sub>.

Inglesfield (1980) also attempted to calculate the effect a smearing of the Fermi distribution ( $\equiv$  raising the temperature) has upon  $\mathbf{D}_2(\mathbf{q})$ . The weak temperature dependence of  $\mathbf{D}_2(\mathbf{q})$  ( $\approx -10\%$  at 630 K) is found not to be sufficient to establish the undistorted structures even at very high temperatures. The conclusion if that is so is that there is a superfluity of soft phonon modes even at high temperatures within these layered TMDs. Consequently *anharmonic* mode-mode coupling effects must play an absolutely essential role in determining the onset transition temperature and above this the lattice dynamics of 'softening' CDW/PLD modes. It would also suggest that the diffuse scattering intensity distributions so often present at high temperatures in CDW/PLD materials may well result from some sort of short-range CDW/PLD distribution, as was originally proposed for 2H-TaSe<sub>2</sub> by McMillan (1976). Such an anharmonic approach to lattice dynamics has been proposed for a wide variety of displacive structural phase transitions (Cowley 1980, A D Bruce 1980, Bruce and Cowley 1980) and in particular for those occurring in SrTiO<sub>3</sub> and LaAlO<sub>3</sub>.

The only theoretical calculation for a layered TMD based upon such an anharmonic strong-coupling approach to date is that of Varma and Simons (1983). Using Inglesfield's simplified band structure for 1T-TaS<sub>2</sub> they calculated  $\mathbf{D}_2(\mathbf{q})$  at  $T = 0$  K and found a maximum of  $-10.5 \text{ eV \AA}^{-2}$  which decreased to  $-8.5 \text{ eV \AA}^{-2}$  at  $T = 100$  K. Using a parameterised short-range contribution it was evident that the transition temperature would be a few thousand degrees if harmonic contributions alone were considered. It

was found that a full anharmonic treatment can suppress this onset transition temperature down to room temperature. Note here that their understanding that 1T-TaS<sub>2</sub> has an *onset* CDW/PLD transition at wave-vector  $q \approx 0.285\Gamma M$  at  $T \approx 350$  K was unfortunately in error. There occurs a phase transition from a high-temperature 1T<sub>1</sub> phase to a nearly commensurate 1T<sub>2</sub> phase at  $\approx 350$  K. The 1CDW 1T<sub>1</sub> phase still contains sharp superlattice spots along the  $\Gamma M$  direction and continues to exist right up to  $\approx 550$  K—the temperature at which the 1T polytype undergoes an inter-polytypic phase transition to a 2H polytype (DiSalvo *et al* 1975, Wilson *et al* 1975). The diffuse scattering distribution that coexists with the sharp superlattice spots from the longitudinal PSD in the 1T<sub>1</sub> phase has been ascribed to partially softened transverse acoustic phonon modes. This being so, it is not so evident that very strong suppression of the onset transition temperature of the longitudinal mode is a feature, particularly in light of the variability of theoretical predictions pertaining to harmonic stability in the layered TMDS. Feldman (1982), it is recalled, suggests that Inglesfield should have used the mass of the metal atom rather than an average mass to convert phonon frequencies to short-range force constants. With just this one simple change the estimated short-range force constant becomes at least  $6.8 \text{ eV } \text{\AA}^{-2}$ , and harmonic stability is attained for 2H-TaS<sub>2</sub>, in contrast to the massive harmonic instability presented by Inglesfield.

The conclusion of this discussion regarding microscopic theoretical calculations must be that, although much has been learnt about the distinctive nature of CDW/PLD phases and phase transitions in the group VB layered TMDS, there remains a long way to go in definitively accounting for what is observed.

## 5. CDW/PLD states characterised by the existence of diffuse intensity distributions

Upon cooling from higher temperatures down towards a transition into some low-temperature three-dimensionally long-range-ordered CDW/PLD state, precursive phenomena are quite often observed in a wide range of physical properties. In particular, diffuse intensity distributions are often found in x-ray and electron diffraction patterns (Pouget 1978, Wilson *et al* 1975); for example, diffuse x-ray patterns are given by quasi-one-dimensional KCP and TTF-TCNQ (Khanna *et al* 1977). These have been understood in terms of dynamical scattering from soft intra-chain phonon modes (Pouget 1978). The scattering is uncorrelated from chain to chain, leading to planar diffuse scattering.

Diffuse scattering is also observed in the 2H layered TMDS. Wilson *et al* (1975) report the existence of weak diffuse streaking between the Bragg spots, and diffuse peaks occur near the  $(\frac{1}{3}, 0, 0)$  wave-vectors of the low-temperature superstructure to well above the ordered state onset transition temperature,  $T_0$ . Here there is little or no correlation between layers as indicated by the two-dimensional diffuse scattering distribution.

In the case of the 1T polytypes the characteristic bicycle-chain pattern of diffuse intensity found in the 1T<sub>1</sub> state coexists with the sharp satellite spots of this incommensurate phase. Such coexistence of sharp CDW/PLD superlattice spots and diffuse streaking has recently been observed again in the CDW/PLD-bearing tetra-telluride NbTe<sub>4</sub> (Eaglesham *et al* 1985a).

The disappearance of diffuse scattering signals the attainment of some lower-temperature phase, bearing a new or greatly improved long-range three-dimensional order, e.g. at rotational lock-in to the  $(13)^{1/2}a_0$  superlattice (and  $13c_0$  stack) in 1T-TaSe<sub>2</sub> at  $T_1 = 473$  K.

From a wide range of phenomena it would appear that dynamical fluctuations (McMillan 1976) play a crucial role in the temperature-dependent behaviour of CDW/PLD systems. The diffuse scattering intensity distributions in reciprocal space thus provide direct information about the detailed form of such fluctuations. Fluctuations above  $T_0$  are of particular interest.

### 5.1. CDW/PLDs and the high-temperature 'undistorted' phase of the 2H polytypes

In a seminal work McMillan (1976) developed a strong-coupling theory of CDW/PLD formation in the 2H polytypes which suggested that the disappearance of sharp CDW/PLD superlattice spotting above the 'onset' temperature,  $T_0$ , was due not to a vanishing CDW/PLD amplitude, but rather to break-up in the long-range phase coherence between CDW/PLD superlattice cells ( $\approx 10 \text{ \AA}$ ). There is above  $T_0$ , within this picture, still a large amplitude to the active phonon mode within individual superlattice cells and a sizable although temporally fluctuating local energy gap.

One might expect such a short-range-ordered fluctuating CDW/PLD distribution to give rise to structured diffuse diffraction effects above onset. As noted earlier such diffuse scattering distributions have been variously reported for the 2H materials (Wilson *et al* 1985, Chevalier and Stobbs 1975, Chen 1984). Unfortunately there has been little systematic study of whether these diffuse scattering distributions are true precursors to the pure-phase static coherent CDW/PLD. Chen (1984) reported a well defined temperature-dependent elliptical contour of diffuse intensity in 2H-NbSe<sub>2</sub> below  $T_0$  at 20 K, in coexistence with sharp  $\frac{1}{2}a_0^*$  and  $\frac{1}{2}a_0^*$  superlattice spots. S McKernan and D J Eaglesham (private communication) report this same diffuse scattering intensity distribution in 2H-NbSe<sub>2</sub> although only above  $T_0$ , and now of course without the sharp superlattice spots.

It is known that the diffuse scattering distributions are strongly affected by impurities and defects (Wilson *et al* 1975, Mutka *et al* 1984). Recently the effects of defects on CDW/PLDs in various TMDs have been systematically studied in a beautiful series of irradiation and EM experiments (Mutka *et al* 1984, 1981). The major conclusion is that the principal effect of defects is to destroy the phase coherence of the CDW/PLD rather than its amplitude. Following McMillan (1975a,b), it is believed that the foreign potential of the defects triggers static local CDW/PLDs with an enhanced onset transition temperature. The random siting of these local CDW/PLDs suppresses the attainment of long-range order, and leads to visible pre-transition effects in electron diffraction. Mutka *et al* (1984) find that the effect of these defects is to broaden the CDW/PLD satellite spots, the diffuse intensity being concentrated around the original satellite positions. Whether such a diffuse scattering distribution bears any relation at all to the elliptical streaked contours of diffuse intensity observed in the 'pure' materials remains far from clear. A coupled diffraction and residual resistivity ratio investigation of the 2H materials above  $T_0$  could be very illuminating.

Other phenomena that reveal precursive behaviour above onset in the various 2H materials are briefly summarised below.

(i) The inelastic neutron study on 2H-TaSe<sub>2</sub> by Moncton *et al* (1977) found above  $T_0$  both the softening phonon side-bands about  $q_0$  at finite frequency and also a quasi-elastic central peak in the soft-mode spectral function  $S(q, \omega)$ . The quasi-elastic central peak developed strongly below about 150 K, and its integrated intensity diverged as  $1/(T - T_0)$ . By 123 K ( $T_0$ ) the in-plane correlation length of the quasi-elastic scattering reaches  $\approx 150 \text{ \AA}$  (or a dozen supercells), while that perpendicular to the plane is  $\approx 45 \text{ \AA}$

(or half a dozen sandwiches). The energy width, however, could not be measured since the spectrometer resolution was not good enough.

(ii) The temperature dependence of the resistivity above onset in 2H-TaSe<sub>2</sub> is found to follow  $\rho = AT + B$  with  $B$  large, whereas that for 2H-NbS<sub>2</sub>, which does not show CDW/PLD instabilities, one simply finds  $\rho \approx AT$  (Naito and Tanaka 1982). Above the Debye temperature, the resistivity of a normal metal is usually proportional to the mean square displacement amplitude,  $\rho \propto \overline{X^2}$ , which in turn is proportional to the temperature (Dugdale 1977). Naito and Tanaka (1982) attribute the extra constant term  $B$  in 2H-TaSe<sub>2</sub> to 'impurity-like scattering from local CDW/PLD fluctuations'.

(iii) Nb NMR studies of 2H-NbSe<sub>2</sub> (Valic *et al* 1975, Stiles and Williams 1976, Berthier *et al* 1978) recorded a pre-transitional broadening above  $T_0$  for the  $m \rightarrow m - 1$  transition ( $m \neq \frac{1}{2}$ ). Stiles and Williams (1976) showed that the temperature dependence of the broadening behaved like  $1/(T - T_0)$ , which was interpreted as being due to dynamical fluctuations of the CDW/PLD. Berthier *et al* (1978), however, concluded that this pre-transitional broadening was due to static fluctuations induced by impurities.

(iv) Ultrasonic/elasticity measurements on 2H-TaS<sub>2</sub> and 2H-TaSe<sub>2</sub> (Barmatz *et al* 1975, Jericho *et al* 1980) found an unusual temperature-dependent reduction in the elastic constant  $c_{11}$  up to around 100 K or so above  $T_0$ . Note, however, the same behaviour was not found with 2H-NbSe<sub>2</sub>, for which the static CDW amplitude is markedly smaller.

(v) The specific heat and resistivity measurements of Craven and Meyer (1977) revealed the presence of strong fluctuations for temperatures either side of  $T_0$  in both 2H-TaSe<sub>2</sub> and 2H-TaS<sub>2</sub>. From a measurement of the excess specific heat above the linear mean-field estimate, Craven and Meyer (1977) assessed the length scale of the fluctuations above  $T_0$  in 2H-TaSe<sub>2</sub> to be  $\approx 14 \text{ \AA}$ .

(vi) A very recent thermal conductivity measurement on 2H-TaSe<sub>2</sub> (Nuñez-Regueiro *et al* 1985) finds an abnormally large phonon contribution to the thermal resistivity to far above  $T_0$ , which is rapidly lost below  $T_0$ . The strong phonon scattering above onset was analysed in terms of a pseudo-spin formulation involving one pseudo-spin per superlattice cell.

The exact nature of the short-range order that apparently exists above onset in the 2H CDW/PLD-bearing materials is clearly an intriguing problem. If simply driven by static impurity-induced fluctuations, it remains to be explained why the quasi-elastic central-peak intensity or the NMR line broadening should vary as  $(T - T_0)^{-1}$ . If the elliptical contours of diffuse scattering turn out to be a genuine precursor effect, it then remains to be understood in detail how either a static random distribution of local CDW/PLDs, or dynamic CDW/PLD excitations, can give rise to such a scattering distribution.

## 5.2. Diffuse scattering below $T_0$ in the 1T polytypes

The incommensurate 1T CDW states (1T<sub>1</sub>-TaS<sub>2</sub> above 350 K, 1T<sub>1</sub>-TaSe<sub>2</sub> above 473 K, and 1T-VSe<sub>2</sub> between 80 and 110 K) each exhibit very similar diffuse scattering intensity distributions, consisting of chain-like patterns of interlocking circles (see figure 9 (plate), and plates in Van Landuyt *et al* 1974, Wilson *et al* 1975, Scruby *et al* 1975, Eaglesham *et al* 1986). The diffuse intensity distribution is accompanied by sharp incommensurate CDW/PLD spots. In the case of 1T<sub>1</sub>-TaS<sub>2</sub> and 1T<sub>1</sub>-TaSe<sub>2</sub> the primary incommensurate spots are embedded in the strong arcs of diffuse scattering. The second-order spots, however, are all separate and sharp. 1T-VSe<sub>2</sub> seems to be somewhat different in that

the diffuse scattering appears not to peak at the same height,  $k_z c^*$ , as the primary CDW/PLD satellite spots (D J Eaglesham, private communication).

The general form of the diffuse intensity distribution is remarkably resistant to the effects of doping (see figure 20 of Wilson *et al* 1975), although the sharp second-order satellite spots are rapidly suppressed. DiSalvo *et al* (1975) found that the lower temperature lock-in transitions were suppressed fairly rapidly by cation doping. When the lock-in transitions disappear, however, the transition temperatures had not yet dropped to zero; instead the transitions, as measured by the resistivity anomalies, had simply faded away. Mutka *et al* (1984) recently have followed in 1T-TaS<sub>2</sub> the way in which the sharp phase transitions are lost as accumulated radiation defects modify the configuration and kinetics of the CDW/PLD. Extrapolating back to 'pure' 1T<sub>1</sub>-TaS<sub>2</sub>, their results would suggest that then the pre-lock-in CDW/PLD condition is dominated largely by intrinsic thermal fluctuations (phasons and amplitudons) as against static fluctuations induced by defects (Mutka *et al* 1984).

The characteristic signature of thermally induced dynamical *phase* fluctuations (phason modes) in an incommensurate CDW/PLD (see Overhauser 1971, Giuliani and Overhauser 1981) has recently been detected in an x-ray diffraction study of 1T-TaS<sub>2</sub> (Chapman and Colella 1984). Following Overhauser (1971) and Wilson *et al* (1975), and ignoring the chalcogen atoms for simplicity, the metal atomic displacements due to a single incommensurate CDW/PLD with wave-vector  $q_0$  can be described by  $U(r_j) = A \sin(q_0 \cdot r_j + \varphi_0)$ , where  $A$  is the PLD amplitude and is parallel to  $q_0$ ,  $r_j$  labels the pre-CDW/PLD atomic positions, and  $\varphi_0$  is a phase angle. For a purely incommensurate CDW/PLD, the phase angle  $\varphi_0$  can suffer fluctuations. Introducing such modes necessitates replacing  $\varphi_0$  by

$$\varphi_0 + \sum_k \varphi_k \sin(\mathbf{k} \cdot \mathbf{r}_j - \omega_k t).$$

The resultant structure factor  $F(\mathbf{g})$  now becomes

$$F(\mathbf{g}) = Nf \sum_{\alpha=-\infty}^{\infty} e^{i\alpha\varphi_0} J_{\alpha}(\mathbf{g} \cdot \mathbf{A}) \prod_k \sum_{\beta=-\infty}^{\infty} J_{\beta}(\alpha\varphi_k) \delta[\mathbf{g} - (\mathbf{G} - \alpha\mathbf{q} - \beta\mathbf{k})] \quad (5.1)$$

where  $N$  is the number of unit cells,  $\mathbf{G}$  represents a reciprocal-lattice vector,  $f$  is an atomic scattering amplitude, and the  $J$ s are Bessel functions of various orders. Clearly one effect of the phasons is to give rise to diffuse scattering at wave-vectors other than  $\mathbf{G} + \alpha\mathbf{q}_0$ . The matrix structure factors,  $F(\mathbf{G}) = NfJ_0(\mathbf{G} \cdot \mathbf{A})$ , are unaffected by the presence of the phason excitations whereas the CDW/PLD structure factors ( $\alpha \neq 0$ ,  $\beta = 0$ ) are strongly affected:

$$F(\mathbf{G} + \alpha\mathbf{q}_0) = F^0(\mathbf{G} + \alpha\mathbf{q}_0) \prod_k J_0(\alpha\varphi_k)$$

where  $F^0$  represents the structure factor in the absence of the thermally induced phason fluctuations. Following Overhauser (1971) this can be rewritten as

$$F(\mathbf{G} + \alpha\mathbf{q}_0) = F^0(\mathbf{G} + \alpha\mathbf{q}_0) \exp\left(-\sum_k \frac{1}{2} \alpha^2 \varphi_k^2\right). \quad (5.2)$$

Equating the average kinetic energy of each phason mode to  $\frac{1}{2}k_B T$  gives  $\mathcal{T}_k = \frac{1}{2}NM\omega_k^2 \varphi_k^2 A^2 = \frac{1}{2}k_B T$  and a temperature-dependent CDW/PLD structure factor

$$F(\mathbf{G} + \alpha\mathbf{q}_0) = F^0(\mathbf{G} + \alpha\mathbf{q}_0) e^{-\alpha^2 CT} \quad (5.3)$$

where

$$C = \sum_k \frac{2k_B}{NM\omega_k^2 A^2}.$$

The squared phason temperature factor  $e^{-2CT}$ , which multiplies the intensity of every first-order satellite, was found to decrease from 0.27 at 360 K to 0.22 at 420 K for  $1T_1$ -TaS<sub>2</sub> (Chapman and Colella 1984). The phason temperature factor was also found to be necessary in order to explain the relative intensities of primary and higher-order CDW/PLD satellite spots. The large ( $\approx 75\%$ ) amount of intensity removed from the primary superlattice spots due to the low-energy dynamic CDW/PLD excitations (both phasons and amplitudons) re-appears in the form of diffuse intensity

$$|F(\mathbf{G} + \mathbf{q}_0 + \mathbf{k})|^2 \propto (\mathbf{g} \cdot \mathbf{A})^2 \varphi_k^2. \quad (5.4)$$

In general, one would expect this diffuse intensity to be peaked in the vicinity of the primary satellite spots. The fact that the strong arcs of diffuse scattering are observed in  $1T_1$ -TaS<sub>2</sub> and  $1T_1$ -TaSe<sub>2</sub> running through the primary satellites suggests that the high-temperature  $1T_1$  state is highly unstable to transverse fluctuations of the CDW/PLD wave-vector directions. One should note that the transverse nature of this instability persists in Ti-doped  $1T$ -(Ta/Ti)S<sub>2</sub> long after the (average) CDW wave-vector has departed from the rotated  $(13)^{1/2}a_0$  lock-in value. In 4Hb and 6R-TaS<sub>2</sub>, (where there are not the *c* axis stacking problems associated with  $1T_1$ -TaS<sub>2</sub>) or VSe<sub>2</sub>, the diffuse scattering above lock-in is much reduced. A detailed inelastic neutron scattering investigation of the dynamic CDW/PLD excitations in  $1T_1$ -TaS<sub>2</sub>, such as that recently performed for incommensurate ThBr<sub>4</sub> (Bernard *et al* 1983), would clearly be of great interest.

## 6. Static CDW/PLD distributions

Upon cooling many CDW/PLD systems undergo a variety of phase transitions where at least some of the higher-temperature diffuse scattering condenses into sharp satellite spots. Such transitions signal 'pinning' of the phase of the CDW/PLD by the underlying lattice. A strong phase transition frequently can be detected through a whole range of techniques. Diffraction experiments in particular reveal within the above general framework a curious variety in the observed behaviour, for there can occur 1D, 2D and 3D pinnings together with multi- and single- $\mathbf{q}$ , high- and low-symmetry states.

There may arise incommensurate states with strong temperature dependences of the CDW/PLD wave-vectors but only very weak higher harmonics, as for the principal CDW/PLD wave-vectors of  $\alpha$ -uranium (Marmeggi and Delapalme 1982, Smith and Lander 1983).

There arise also states that are nearly commensurate (NC), characterised by wave-vectors that are nearly independent of temperature and yet that show strong higher harmonics of the fundamental wave-vectors. An example is the NC  $1T_2$  phase of  $1T$ -TaS<sub>2</sub> (Yamada and Takatera 1977). Also the triple- $\mathbf{q}$  'incommensurate' phase of  $2H$ -TaSe<sub>2</sub> becomes rather like this well away from onset (Moncton *et al* 1977). Such non-sinusoidal states sometimes prove to be 'discommensurate' (McMillan 1976).

There further appear 'incommensurate' states having completely temperature-independent CDW/PLD wave-vectors but weak harmonics, as with both of the quite separate CDW/PLDs observed in NbSe<sub>3</sub> (Fleming *et al* 1984), or with the double- $\mathbf{q}$  state of  $1T$ -VSe<sub>2</sub> occurring below 85 K (Eaglesham *et al* 1986, Bird *et al* 1985). Note this low-

**Table 1.** A survey of incommensurate behaviour. 2H-TaS<sub>2</sub> seems to behave like 2H-NbSe<sub>2</sub> but its wave-vector is now of magnitude greater than  $\frac{1}{3}$ , not smaller (Scholz *et al* 1982).

	Weak or zero harmonic content to IPLD/CDW	Medium or strong harmonic content to IPLD/CDW
Weak or zero temperature dependence of wave-vector	NbSe <sub>3</sub> (O and Y) NbTe <sub>4</sub> $\eta$ -Mo <sub>4</sub> O <sub>11</sub> KCP VSe <sub>2</sub> ( <i>c</i> component) [Ta(Se <sub>2</sub> ) <sub>2</sub> ]I	1T <sub>2</sub> -TaS <sub>2</sub> 2H-TaSe <sub>2</sub> (NbSe <sub>2</sub> ) (well away from onset)
Strong temperature dependence of wave-vector	$\alpha$ -U TaS <sub>3</sub> K <sub>0.3</sub> MoO <sub>3</sub>	2H-TaSe <sub>2</sub> (NbSe <sub>2</sub> ) (close to onset)

temperature state of 1T-VSe<sub>2</sub>, as with that of 1T<sub>2</sub>- or 1T<sub>3</sub>-TaS<sub>2</sub>, does not present the simplicity of the  $(13)^{1/2}a_0 \times (13)^{1/2}a_0 \times 13c_0$  condition gained by 1T-TaSe<sub>2</sub>. The latter commensurate PLD nonetheless is noteworthy in that it is strongly non-sinusoidal, as is revealed directly by diffraction and indirectly through Mossbauer, NMR, TDPAC etc.

The various forms of observed incommensurate behaviour are summarised in table 1. Some details will now be discussed.

### 6.1. Temperature-independent incommensurability

The phenomenon of temperature-independent incommensurability within CDW/PLD systems is intriguing because it raises fundamental questions about incommensurability, discrete lattice effects and the validity of Landau-like free-energy expansions (McMillan 1975a,b, Cowley 1980).

Within the usual Landau-like free-energy approach, the finally adopted incommensurate CDW/PLD wave-vector is determined by the competition between 'lock-in' free-energy terms, which favour some nearby commensurate ordering, and 'elastic' gradient terms, which favour retention of some incommensurate wave-vector. The 'lock-in' free-energy terms are generally of higher order in the appropriate order parameter than are the harmonic gradient terms, and consequently any change in the CDW/PLD amplitude as a function of temperature ought to lead to a change in wave-vector (Moncton *et al* 1977, McMillan 1975a,b). One might, of course, artificially arrive at temperature-independent CDW/PLD wave-vectors either by making the coefficients of the appropriate gradient terms excessively large, or, conversely, by making the coefficients of the lock-in terms excessively small. There appears, however, to be very little microscopic justification for either circumstance—except perhaps for the case of an extremely anisotropic one-dimensional CDW/PLD, where a divergent  $\chi^0(\mathbf{q} = 2\mathbf{k}_F)$  would produce a strongly defined CDW/PLD wave-vector component along the chain direction. Such a situation does not apply, however, to the two temperature-independent incommensurate CDW/PLD wave-vectors observed in NbSe<sub>3</sub> (below 144 and 59 K respectively; Fleming *et al* 1978). The ratios of the correlation lengths parallel and perpendicular to the chain direction are (as obtained from x-ray diffuse scattering measurements above the respective onset transitions) only  $\approx 5$  (Fleming *et al* 1978). Why then do the CDW/PLDs in NbSe<sub>3</sub> cling so tenaciously to their incommensurate values of  $\mathbf{q}_1 = (0, 0.2412, 0)$

and  $q_2 = (0.5, 0.2604, 0.5)$  (Fleming *et al* 1984)? Turning to the alternative extreme possibility, one must ask why it is that the  $\approx 2.7\%$  'incommensurate' CDW/PLD state in 2H-TaSe<sub>2</sub> should near onset be so sensitive to third-order lock-in free-energy terms, whereas the incommensurate CDW/PLDs in NbSe<sub>3</sub> appear quite unresponsive to the approximately  $3\frac{1}{2}\%$  deviation in their wave-vectors withholding fourth-order lock-in?

A similar puzzle is set by the contrast in behaviour of the CDW/PLD wave-vectors in 1T-VSe<sub>2</sub> (Moncton *et al* 1977, Tsutsumi 1982) with those in 1T-TaSe<sub>2</sub>. In the latter material at lock-in the basal-plane components of the wave-vectors rotate  $\approx 13.9^\circ$  away from the  $\Gamma M$  direction, while the wave-vector components perpendicular to the sandwiches jump substantially away from their high-temperature preferred value of  $\frac{1}{3}$  to the superlattice stack value of  $\frac{2}{3}$ —all to obtain fourth-order lock-in free energy. By contrast in 1T-VSe<sub>2</sub> the CDW/PLD wave-vectors appear not to be impelled to alter their components perpendicular to the layers (0.314), whether by the  $-20\%$  or so required for lock-in to  $(\frac{1}{4}, 0, \frac{1}{4})$  and the resultant fourth-order lock-in free-energy gain, or by the  $+6\%$  required to lock-in to  $(\frac{1}{4}, 0, \frac{1}{3})$  and a gain of the third order ( $q_1 + q_2 + q_3$ ) lock-in free energy (Tsutsumi 1982).

A further apparent example of temperature-independent incommensurability is provided by the incommensurate phase of the recently investigated semi-chain compound NbTe<sub>4</sub> (Boswell *et al* 1983, Mahy *et al* 1982, 1984, 1985, Eaglesham *et al* 1985a). Once again a Landau theory approach predicts a temperature-dependent incommensurability (Sahu and Walker 1985). The experimental evidence so far, however, suggests that the incommensurability parameter  $\delta$  remains fixed at 0.022 all the way down from room temperature to the lock-in at  $\approx 50$  K (Mahy *et al* 1984, 1985, Eaglesham *et al* 1985a). There has, though, as yet been no really accurate x-ray study of the temperature dependence of  $\delta$ . It might also be pointed out that electron microscope work reveals the 50 K phase transition to be extremely sluggish, it taking nearly an hour from start to finish (Eaglesham *et al* 1985a), this being the slowest CDW/PLD lock-in transition yet reported. It would be interesting to see more transport measurements as a function of temperature for NbTe<sub>4</sub>.

What effect might pin the incommensurate CDW/PLD wave-vectors in NbSe<sub>3</sub> (Fleming *et al* 1984), or in the double- $q$  state of 1T-VSe<sub>2</sub> below 85 K (Tsutsumi 1982, Eaglesham *et al* 1985a) or in the incommensurate state of NbTe<sub>4</sub> (Mahy *et al* 1984, 1985, Eaglesham *et al* 1985a)? One possibility is some sort of impurity pinning (Bak *et al* 1985), but in consequence there should be broadened satellite spots and shortish coherence lengths. For the case of NbSe<sub>3</sub> recent synchrotron measurements reveal by contrast a coherence length along the chain direction in excess of 4000 Å (Fleming *et al* 1984). In the case of 1T-VSe<sub>2</sub> there is some evidence that poor stoichiometry could play some sort of role. Crystals are often found with excess vanadium in the van der Waals gap between the sandwiches, and such defects are known to affect CDW/PLD formation (DiSalvo and Waszczak 1981). However, the sharpness of the satellite spots in VSe<sub>2</sub> (Tsutsumi 1982) and the large size of the well defined double- $q$  domain structures recently observed (from about 1000 Å to a few  $\mu\text{m}$ —see Eaglesham *et al* 1986) indicate that impurity pinning plays only a minor role in the best samples of 1T-VSe<sub>2</sub>. Likewise, satellite dark-field imaging of NbTe<sub>4</sub> indicates coherence over micrometres (Eaglesham *et al* 1985a), which again rules out impurity pinning as the source of the temperature-independent incommensurability.

The nearest low-order rational fractions consistent with the experimentally observed incommensurate wave-vector components in NbSe<sub>3</sub> are  $\frac{1}{4}\frac{27}{28}$  for  $q_1$  and  $\frac{1}{4}\frac{25}{24}$  for  $q_2$  (Wilson 1981, 1985a). To stabilise such wave-vectors a conventional Landau theory approach

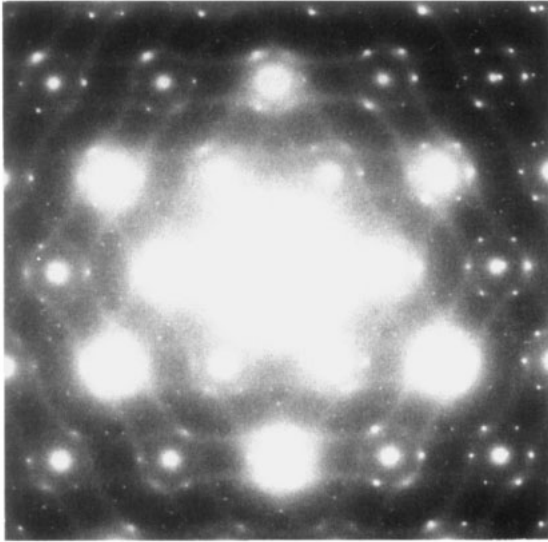


**Figure 9.** Electron diffraction from 1T-TaS<sub>2</sub> in its symmetric ICdW state (between 350 and 190 K when cooling), showing the coexistence of sharp spots and arcs of diffuse scattering.



would require an expansion to orders 112 and 96 respectively in the CDW/PLD order parameter! In  $VSe_2$  the nearest low-order rational fractions consistent with the two CDW/PLD wave-vectors observed below 85 K are  $q_1 = \frac{1}{4}a^* + \frac{4}{13}c^*$  and  $q_2 = \frac{1}{4}(-a^* + b^*) + \frac{4}{13}c^*$ . An expansion to order 52 would be required to lock-in the wave-vector component parallel to  $c^*$ . In  $NbTe_4$  the nearest low-order rational fraction to the incommensurability parameter  $\delta = (0.0220 \pm 0.002)$  is  $\frac{1}{48}$ , thus giving CDW/PLD wave-vector  $q_1 = \frac{1}{2}a^* + \frac{1}{2}b^* + \frac{11}{48}c^*$ ,  $q_2 = \frac{11}{48}c^*$ , and  $q_3 = \frac{1}{48}c^*$  (Eaglesham *et al* 1985a). Again a very high commensurability order (16) is required.

In using Landau theories used to discuss CDW/PLD phases in both the 2H (Jacobs and Walker 1980) and 1T (Nakanishi and Shiba 1984) layered compounds it has usually been found possible to explain qualitatively the observed behaviour with free-energy expansions out only to fourth-order in the order parameter. However, in order to explain the existence of a double- $q$  CDW/PLD state in 1T- $VSe_2$  a recent Landau theory has required the inclusion of at least sixth-order terms (Eaglesham *et al* 1986). Little is known quantitatively about the rate of convergence of such free-energy expansions as a function of the order parameter exponent. If one uses a typical and roughly normalised metal atom PLD amplitude (i.e.  $\approx 0.1 \text{ \AA}/1 \text{ \AA} = 0.1$  (Bird and Withers 1985)) as an order parameter, then  $(0.1)^n$  gives an estimate of how rapidly free-energy contributions diminish with commensurability order for purely incommensurate systems. Clearly the commensurability orders apparently required for  $NbSe_3$ , 1T- $VSe_2$  and  $NbTe_4$  cannot be stabilised by purely sinusoidal CDW/PLD distortions.

If, on the other hand, the distortions are strongly non-sinusoidal or are discommensurate, then additional free-energy contributions arise that may not be so negligible. This will depend upon how quickly the amplitudes of higher harmonics fall off. In the case of 2H-TaSe<sub>2</sub> just prior to lock-in the amplitude ratio of the second harmonic to the primary harmonic has risen to  $\approx 0.3$ , with a 'normalised' metal atom amplitude  $\approx 0.05/1.0$  (Moncton *et al* 1977).

Consider a primary CDW/PLD with wave-vector  $q$  such that  $2nq \in G$ , a reciprocal-lattice vector. The contribution of the primary harmonic to the pinning energy is then  $F_1 = (A_1)^{2n}$ , whereas that of the second harmonic  $2q$ ,  $n(2q) \in G$ , is given by  $F_2 = (A_2)^n$ . The ratio of the two contributions  $F_2/F_1$  is equal to  $(A_2/A_1)^n/A_1^n$ . Using the above example  $A_2/A_1 = 0.3$  and  $A_1 = 0.05$ , and it is easy to see that the contribution of the second harmonic will be much more significant. When there exist a whole string of harmonics there will also exist a huge number of such terms. Clearly discommensurate distortions may be able to pin higher-order commensurate wave-vectors, whereas purely sinusoidal distortions are most unlikely to (Bruce and Cowley 1980). If the widths of the discommensurations or solitons (see below) systematically produced in such a non-sinusoidal distortion are not large in comparison with the underlying lattice spacing, it is clear that a continuum-based Landau free-energy approach must be abandoned and a Devil's Staircase approach (Bak 1982, Aubry 1983) taken up. In such a case any sharp discommensurations might be expected to be centred on a particular point within the unit cell, and so give rise to a quantisation of the CDW/PLD wave-vector (Bruce *et al* 1980, D A Bruce 1980).

Wilson (1985, 1982) developed a weakly discommensurate model for  $NbSe_3$  and Eaglesham *et al* (1985a) have proposed this type of model in order to explain the temperature-dependent incommensurability in  $NbTe_4$ .  $NbTe_4$  is clearly strongly non-sinusoidal, and hence a high-order commensurate picture should be appropriate in this case. For  $NbSe_3$  and 1T- $VSe_2$  the diffraction evidence points to a much lower level of non-sinusoidality. Although 4% incommensurability does not sound large it places the

discommensurations in  $\text{NbSe}_3$  only 24 atoms or  $6\lambda$  apart through the relation

$$L_D/a_0 = 1/\delta.$$

It ought to be noted that in  $\text{NbSe}_3$  the discommensurations are viewed however as being charged ( $e/2$ ) due to charge transfer between chains that even in the pre-distorted state are structurally inequivalent (Wilson 1982, 1985a,b).

### 6.2. Non-sinusoidality and discommensurations

The phenomenon of the discommensuration (DC) arises repeatedly in systems with competing periodicities in many branches of condensed matter physics (Bak 1982). In CDW/PLD systems the two competing interactions are the elastic gradient terms, which favour the incommensurate periodicity, and the local 'lock-in' terms, which favour some nearby commensurate periodicity. When the elastic gradient term dominates, the CDW/PLD is characterised by the presence of higher-order harmonics of the primary CDW/PLD wave, induced by anharmonic 'lock-in' terms (Bruce *et al* 1978, Kotani and Harade 1980). McMillan (1976) showed that this series of harmonics builds up a ground state consisting of regions with essentially commensurate character separated by regions across which the positioning of the commensurate order with respect to the underlying lattice slips by a lattice repeat (see figures below). The width of these 'discommensurations' in comparison with the underlying lattice parameter is governed by the relative influence of the 'lock-in' and gradient free-energy terms. It is only as very small incommensurability values,  $\delta$ , are reached that one might expect sharp discommensurations. How well does this one-dimensional picture apply to real CDW/PLD systems?

### 6.3. Discommensurations and 2H-TaSe<sub>2</sub>

The layered TMD 2H-TaSe<sub>2</sub> undergoes a very weakly first-order onset phase transition from the 'normal' state to a triple- $q$  incommensurate CDW/PLD state at 122 K, followed by a further transition into a triple- $q$  commensurate CDW/PLD state at  $\approx 90$  K (Fleming *et al* 1980, Moncton *et al* 1977). The commensurability conditions that hold in the commensurate phase are  $q_1 + q_2 + q_3 = 0$ ,  $3q_1 = a^*$ ,  $3q_2 = b^* - a^*$ , and  $3q_3 = -b^*$ . On warming from the commensurate phase there is a transition into an incommensurate striped phase at 93 K, followed by a transition back into the triple- $q$  incommensurate phase at 112 K. The striped phase is still in fact a triple- $q$  state, but one where only two of the above commensurability conditions hold, namely  $q_1 + q_2 + q_3 = 0$ , and  $3q_1 = a^*$  (see figure 10).

Unlike in the simple one-dimensional case there are now several phase-dependent anharmonic interactions including a phase-dependent inter-sandwich interaction (Jacobs and Walker 1980). The phasings within the commensurate CDW/PLD patches of a strongly discommensurate distortion are *not* determined solely by the in-plane  $3q_j$  'lock-in' interactions (Bird and Withers 1985).

Both the striped and symmetric incommensurate states are discommensurate in the sense that they contain higher harmonics of the primary CDW/PLD wave-vectors which appear to be induced as above by anharmonic interactions. For example, in the symmetric state, where the primary CDW/PLD wave-vectors are given by  $q_j = \frac{1}{3}(1 - \delta)G_j$ , Moncton *et al* (1977) noted that third-order lock-in energy could be gained by inducing second harmonics as observed with *reduced* wave-vector  $q'_j = \frac{1}{3}(1 + 2\delta)G_j$  since  $2q_j +$

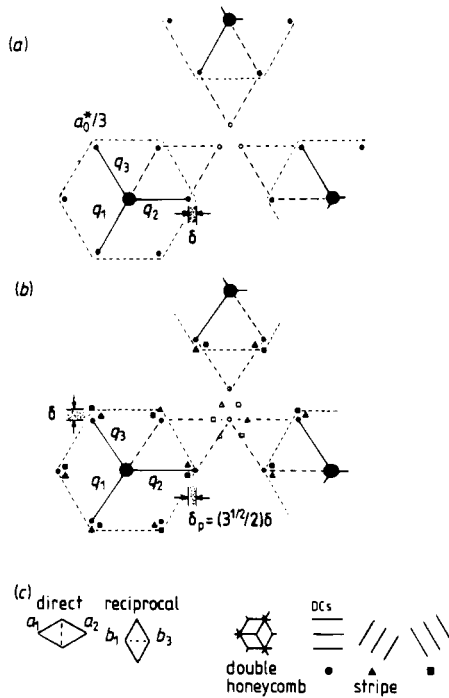


**Figure 10.** The x-ray diffraction patterns observed for the ICDD states of 2H-TaSe<sub>2</sub>: (a) symmetric phase; (b) striped phase (after Fleming *et al* 1980). In the striped phase the variously oriented domains lead to the sets of satellite spots denoted by ●, ■ or ▲. Note that for neither phase was any additional spot splitting recorded, although both phases are now known to involve orthorhombic symmetry breaking (Fung *et al* 1981). Note too that although  $\delta$  between the two states rotates by 30° the discommensurations that result lie parallel—see part (c).

$q'_j = G_j$ . Note that the existence of the harmonic becomes evidence of a discommensurate distortion only when as here the phonon eigenvector of the second harmonic reduces to being almost identical to that of the primary harmonic. In principle anharmonic interactions might also induce phonon modes with reduced wave-vectors in the vicinity of  $O$  or  $q_j - q_{j+1}$ . However, within a soft-mode picture one would not expect these modes to be excited appreciably since their fundamental frequencies are far from being soft (except, of course, for acoustic modes with near-zero wave-vector). The validity of the soft-mode picture for 2H-TaSe<sub>2</sub> is nicely reaffirmed in the recent EM-based determination of its commensurate superstructure (Bird *et al* 1985). Although the most general atomic displacement pattern consistent with the observed orthorhombic space group would permit the existence of displacement waves with wave-vectors  $O$ ,  $\frac{1}{3}G_j$ , and  $\frac{1}{3}(G_j - G_{j+1})$ , in fact only those waves with wave-vector  $\frac{1}{3}G_j$  and longitudinal  $\Sigma_1$  symmetry are found to possess a finite amplitude.

Moncton *et al* (1977) observed in the incommensurate phase that the amplitude of the second harmonic relative to the primary grows from zero near onset to  $\approx 0.3$  just prior to lock-in. This suggests a steady change from a purely incommensurate, sinusoidal distortion near onset to a more strongly discommensurate distortion near lock-in. What is the character of the discommensurate structure just above lock-in? This obviously depends upon the number of higher harmonics induced by the anharmonic interactions, and upon their relative amplitudes and phases. Clearly while the strongest induced

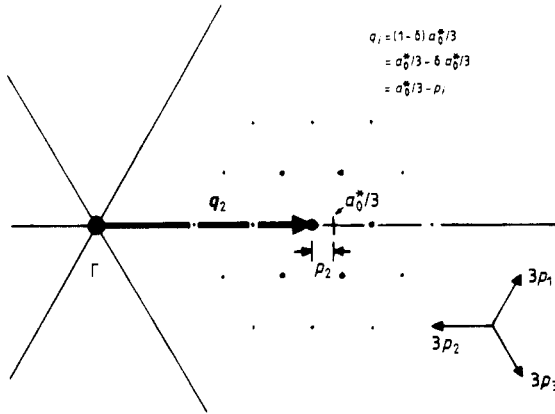


**Figure 11.** The mesh of incommensurate satellite spots predicted for the symmetric IPSD state of 2H-TaSe<sub>2</sub>, spaced by  $\delta_1 a_0^*$ , where  $q_1 = (1 - \delta) a_0^* / 3$ . (After Nakanishi and Shiba 1978.)

harmonic will be the observed second-order harmonic, other higher-order harmonics can also be induced. For example, the  $(q_1 + q_2 + q_3)$  anharmonic interaction could induce a harmonic  $q_3'' = \frac{1}{3}(-b^*) + \frac{1}{3}\delta(2a^* - 2b^*)$ , obeying  $q_1 (= \frac{1}{3}(1 - \delta)a^*) + q_2 (= \frac{1}{3}(1 + 2\delta)(b - a)) + q_3'' = 0$ . Nakanishi and Shiba (1978a,b) showed that, in general, there should be a two-dimensional triangular lattice of higher-order harmonics

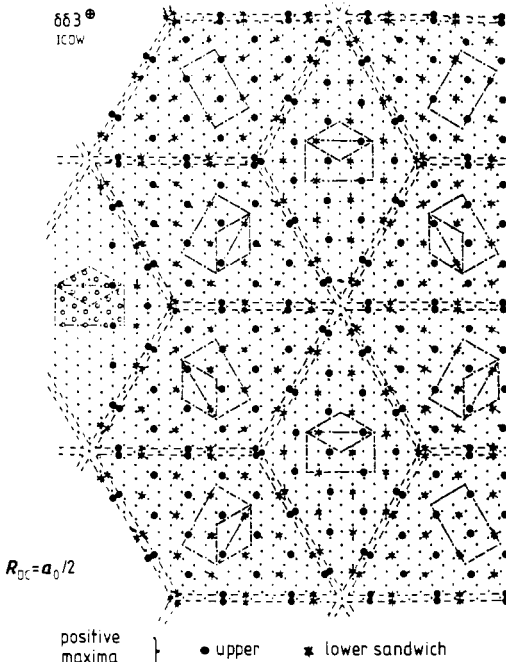


**Figure 12.** The idealised double honeycomb array of discommensurations for the symmetric ICDW state of 2H-TaSe<sub>2</sub>. The orthorhombicity in the ‘commensurate’ patches of this phase is indicated by the rectangular cells. The orthorhombic phasing of the CDW has been idealised to  $\delta\delta_3^{\oplus}$  (see Wilson 1985b). Across each DC the charge maxima shift in both sandwiches perpendicular to the DCs by  $a_0/2$ , causing a switch in orthorhombic orientation. For the actual determined orthorhombic PSD of the commensurate phase, see figure 14. (The orientation corresponds to figure 10 and 11.)

induced around the position of the primary incommensurate satellite spot (see figure 11). The amplitudes of these induced harmonics, however, will decrease rapidly as  $q_h$  moves away from the minimum in the high-temperature soft-mode dispersion. For 2H-TaSe<sub>2</sub> experimentally only the second harmonics  $2q_i$  have been observed in addition to the  $q_i$  and  $q_i - q_j$ .

The recent structural determination of the orthorhombic commensurate state (Bird *et al* 1985) permits a qualitative picture to emerge of the structural adjustments across the discommensurations in 2H-TaSe<sub>2</sub>. For ease of illustration it is customary to draw the DCs as atomically sharp boundaries, which in all probability does not apply to 2H-TaSe<sub>2</sub> at any temperature. A commensurate triple  $q$  atomic displacement pattern is describable by reference to its points of common phasing (Wilson 1978, Wilson and Vincent 1984, Wilson 1985b, Bird and Withers 1985), and the discommensurations follow in terms of rigid shifts in the positions of these points. Figure 12 illustrates, in the idealised infinitely sharp DC limit, the movements of the common phasing points within the two sandwiches of the 2H structure across the distortion boundaries, phase slip being perpendicular to the  $\{11\bar{2}0\}$  lattice directions.

By means of satellite dark-field imaging Fung *et al* (1981) and Chen *et al* (1982) detected just such arrays of 'twin' boundaries, in both the symmetric and striped incommensurate states of 2H-TaSe<sub>2</sub> (figure 13). For both states the individual boundaries are similar, only their geometry of arrangement being different—a double honeycomb array in the symmetric state, and a linear array in the striped state. The remarkable dynamics (McKernan *et al* 1982) and the wealth of microstructure observed, along with the appropriate temperature dependence of the average boundary separation distance, strongly support their interpretation as discommensuration arrays (Fung *et al* 1981). A recent high-resolution synchrotron study of the striped state has provided further support

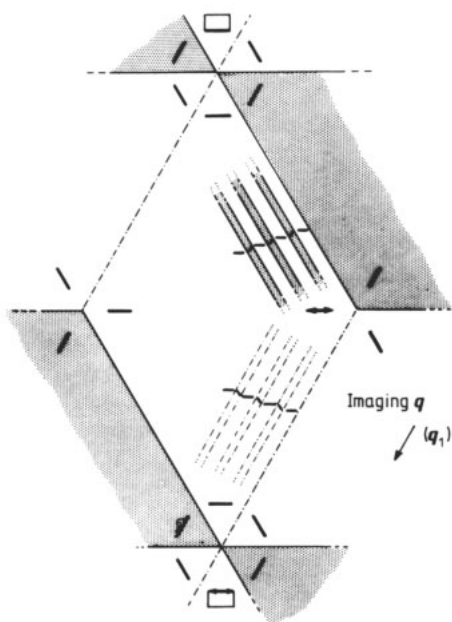


**Figure 13.** Stripe phase DCs ('stripples') nucleating in residual double-honeycomb geometry domains when warming 2H-TaSe<sub>2</sub> back above 90 K. The bars indicate the long axes of the orthorhombic cells: the shading shows the EM contrast obtained for the given DF imaging vector.

for the preceding DC interpretation (Fleming *et al* 1984). It should be noted here that the high visibility of the discommensurations in 2H-TaSe<sub>2</sub> rests on the fact that the commensurate state of the material proves to be orthorhombic, not hexagonal. The images of the 'DC arrays' obtained in the electron microscope by dark-field imaging in  $q_0$  are dominated by the areal contrast from the orthorhombic domains, not line contrast around the DCs themselves (for details see Fung *et al* 1981). Concerning what induces the orthorhombic nature of commensurate 2H-TaSe<sub>2</sub>, we currently have somewhat divergent opinions (see Wilson and Vincent 1984, Wilson 1985b, Bird and Withers 1985).

An important step forward now will be to determine the discommensuration width as a function of temperature via high-resolution electron microscopy. Just this sort of information has been obtained in the case of anti-phase boundaries in compositionally modulated alloys (Terasaki 1982). Interpretation of such high-resolution images is however very difficult. Dynamical diffraction from a discommensurate or even an incommensurate state clearly is capable of generating spurious fringes *ad nauseam* (Steeds *et al* 1986).

Undoubtedly further work is required to establish completely the interpretation that has been offered of the incommensurate phases of 2H-TaSe<sub>2</sub>. This is particularly so at higher temperatures, where one might expect to be tending towards a sinusoidal distortion. Nonetheless the present experimental electron microscope observations do greatly encourage one to use the discommensurate approach in other incommensurate-commensurate phase transition studies. McWhan *et al* (1981) have shown that in 2H-TaSe<sub>2</sub> (where  $q_i < \frac{1}{3}$ ) the DC tend to set perpendicular to a tensile stress axis.

#### 6.4. Inter-sandwich interactions in the commensurate superstructures

The recent determination of the commensurate superstructure in 2H-TaSe<sub>2</sub> at 60 K (see figure 14) manifests strong orthorhombic symmetry within *each* sandwich. In the absence

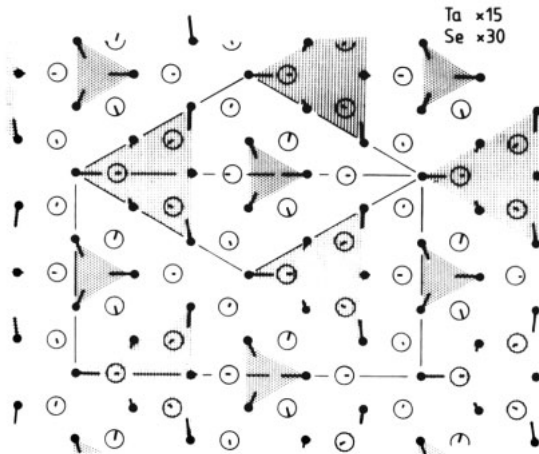


**Figure 14.** The commensurate orthorhombic PSD as determined for 2H-TaSe<sub>2</sub> by electron microscope holz ring intensity analysis (Bird *et al* 1985). The origin has been shifted to permit comparison with the  $\delta\delta3^{\oplus}$  structure given by Wilson (1985b, figure 8) (and in figure 12 above). The triangular cation clusters are shaded. Note this structure yields a pseudo-hexagonal array of diffraction spots. Averaging over domains secures pseudo-hexagonal intensities also, as when working with a large sample in neutron work.

of inter-sandwich interactions, intra-sandwich superstructure symmetry would, it was long assumed, remain trigonal or hexagonal (see Jacobs and Walker 1980). Adopting such a viewpoint, the inter-sandwich interactions appear to play a far more crucial role in the selecting of a specific phasing of the CDW/PLD onto the basal lattice in 2H-TaSe<sub>2</sub> than was previously presumed (Bird and Withers 1985). In 2H they are viewed as securing a  $\delta$ -type orthorhombic structure, in contrast to earlier considered possibilities among orthorhombically stacked  $\beta\beta$  and  $\gamma\gamma$  structures (see Wilson 1985b). Despite the displacement pattern within each sandwich now being orthorhombic, the three axial waves even in the stripe state remain of sufficiently similar amplitude that overall the unit cell retains a pseudo-hexagonal shape.

For 1T-TaSe<sub>2</sub> the  $3a \times b \times 13c$  commensurate superstructure has been taken to be characterised by an identical CDW/PLD structure within each sandwich shifted by stacking vector  $2a + b + c$  from one sandwich to the next. An x-ray diffraction study (Brouwer and Jellinek 1980) indicated that Ta atomic displacements within each hexagonal sandwich lead to a star-shaped cluster pattern, with each star containing 13 Ta atoms in three inequivalent sites with population ratio 1:6:6 (see figure 15). This long-presumed

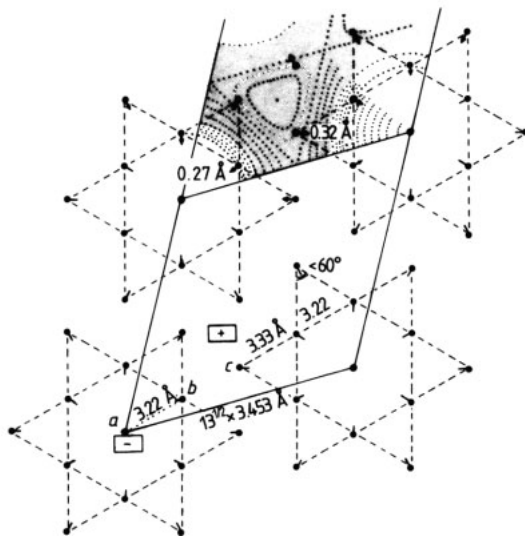


**Figure 15.** The in-plane cation displacements for the  $(13)^{1/2}a$  CCDW of 1T-TaSe<sub>2</sub>, as determined by Brouwer and Jellinek (1980, 1978). In the 13-atom star clusters being formed, the outer ring of six atoms is displaced *more* than the inner ring of six, which by reference to the charge contour lines (from Wilson *et al* 1975) reveals a strong non-sinusoidality for this large-amplitude CPSD. Inter-sandwich coupling will lead also to some triclinicity, not evident in the x-ray work because of domain formation.

pattern of the intra-sandwich distortion has been supported microscopically in measurements of 4f x-ray photo-emission (Hughes and Pollak 1976), TDPAC (Butz *et al* 1979) and the Mossbauer effect (Pfeiffer *et al* 1984). However, a very recent high-resolution NMR and NQR study by Naito *et al* (1985a,b) on the <sup>181</sup>Ta nuclei would appear to detect seven inequivalent Ta sites, and they conclude that fairly strong inter-sandwich coupling must be active in the triclinic stack to shift the intra-sandwich structure significantly away from hexagonal symmetry. Inter-sandwich interactions must then play a significant role in determining the final commensurate state of the CDW/PLD in the case of 1T-TaSe<sub>2</sub>, in like fashion to 2H above. It is again worth pointing out that the sandwich lattice parameters remain pseudo-hexagonal even in the high-amplitude 1T CCDW.

6.5. Discommensurations and 1T-TaS<sub>2</sub>

The octahedral polytype 1T-TaS<sub>2</sub> has, like 2H-TaSe<sub>2</sub>, two distinct ‘nearly commensurate’ incommensurate phases, each characterised by sharp satellite spots (perpendicular and also parallel to the *c*\* axis) and by the presence of strong higher-order harmonics of the fundamental wave-vectors (Nakanishi *et al* 1977, Brouwer 1978, Brouwer and Jellinek 1980, Yamamoto 1983, Tanda and Sambongi 1985). All the satellite spots of either phase can be expressed in terms of a matrix reflection *G* plus appropriate linear combinations of the three fundamental distortion wave-vectors  $q_j = (q^c + \delta_{j\perp}) + q_{jz}c^*$  (*j* = 1, 2, 3). The  $\delta_{j\perp}$ s here monitor the small deviations from basal-plane commensurability, while the basal-plane components of the commensurate vectors satisfy the geometry  $3q_{j\perp}^c - q_{j+1,\perp}^c = G_{\perp}$  (see figure 16). The NC 1T<sub>2</sub> phase, which occurs on cooling between 350 and ≈190 K, but on warming only between ≈280 and 350 K, is

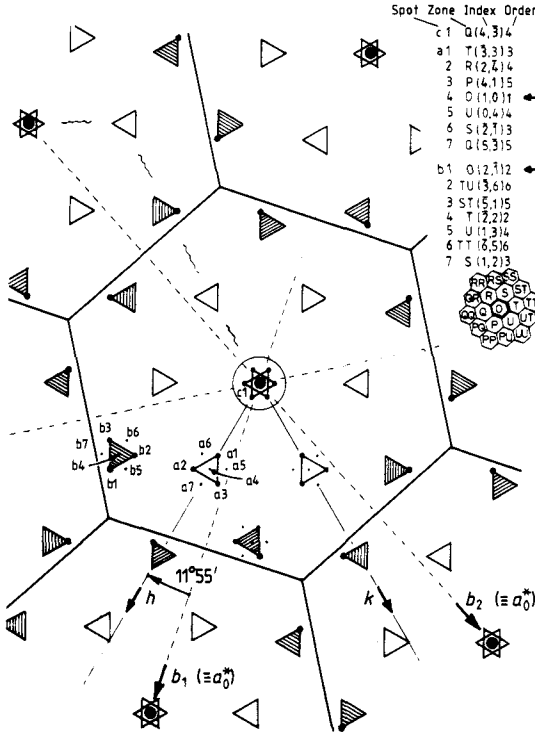


Figure 16. The complex diffraction pattern from 1T<sub>2</sub>-TaS<sub>2</sub>, here slightly idealised as for an 18 × 5 supercell ( $\theta = 11^\circ 55'$ ,  $q_i = 0.2864a_0^*$ ). The high-order indexing of the spot types indicated in the first Brillouin zone is shown top right. For untilted specimens second-order spots b1, which lie in the basal plane, appear stronger than primary spots a4, which sit alternately at  $+c_0^*/3$  and  $-c_0^*/3$ .

characterised by threefold symmetry with respect to the wave-vector positions ( $C_3^+ \delta_{j\perp} = \delta_{j+1,\perp}$ ;  $q_{jz} = \frac{1}{3}$ ) and by the three-dimensional commensurability condition  $q_1 + q_2 + q_3 = c^*$ . The more recently discovered T phase (Fung *et al* 1980, Tanda *et al* 1984, 1985) which is found when warming between ≈220 and 280 K is characterised by broken threefold symmetry in regard to its wave-vector positions ( $C_3^+ \delta_j \neq \delta_{j+1}$ , yet with  $\delta_{1\perp} + \delta_{2\perp} + \delta_{3\perp} = O$ ). It shows also a very close proximity to the three-dimensional commensurability condition  $3q_1 - q_2 = a^* + c^*$  (note that at  $T = 225$  K,  $q_{1z} = 0.439$ ,  $q_{2z} = 0.319$  and  $q_{3z} = 0.242$ ).

In both the above phases harmonics of the fundamental distortions are induced so as to take advantage of fourth-order lock-in free energy, implicit in the commensurability condition  $3q_j - q_{j+1} = \mathbf{G}$ . For example within the NC  $1T_2$  phase a harmonic  $q'_j = -2q_j + q_{j+1}$  is induced that occurs within the same region of reciprocal space as the fundamental  $q_j$  when projected onto the basal plane; its component parallel to  $\mathbf{c}^*$ , however, is  $-\frac{1}{3}$  while that of the  $q_j$  is  $+\frac{1}{3}$ . It is the experimental presence of strong harmonics of this type that has prompted discommensurate modelling of  $1T_2$ -TaS<sub>2</sub> (Nakanishi and Shiba 1977, Nakanishi *et al* 1977). In general a structure may properly be described as discommensurate only when the corresponding PLD eigenvectors for waves  $q_j$  and  $q'_j$  are very similar.

The 'commensurate'  $1T_3$  phase of TaS<sub>2</sub> finally gained upon cooling below  $\approx 190$  K, and which is retained up to  $\approx 220$  K when warming, is characterised by satellite spots that are commensurate and sharp within the basal plane, but that are very broad parallel to  $\mathbf{c}^*$  (Tanda *et al* 1984). This terminal state (unlike for  $1T$ -TaSe<sub>2</sub> which is well ordered) cannot be described in terms of three-dimensional wave-vectors. This fact further impairs a direct description of either the NC  $1T_2$  or the T phase in terms of discommensurations separating regions of the 'commensurate'  $1T_3$  structure.

Nakanishi and Shiba (1977, 1984) have presumed a two-dimensional network of discommensurations separating regions of commensurate  $(13)^{1/2} \times (13)^{1/2}$  superstructure within individual sandwiches for both the  $1T_2$  and T phases. The size and shape of the proposed DC networks is governed then by the incommensurability parameters  $\delta_{j\perp}$ . In the case of the NC  $1T_2$  phase, the proposed DC network is a single honeycomb array, whilst in the T phase it is a stretched honeycomb network. The observed wave-vector components parallel to  $\mathbf{c}^*$  are next postulated to be obtained by the appropriate regular stacking of this much larger commensurate domain structure. In the case of the NC  $1T_2$  phase, the experimental  $\mathbf{c}^*/3$  vector would call then for rhombohedral packing of a virtually regular discommensurate basal-plane domain structure, and give in projection a triple-honeycomb array of DCs (Walker and Withers 1983) (see figure 17).

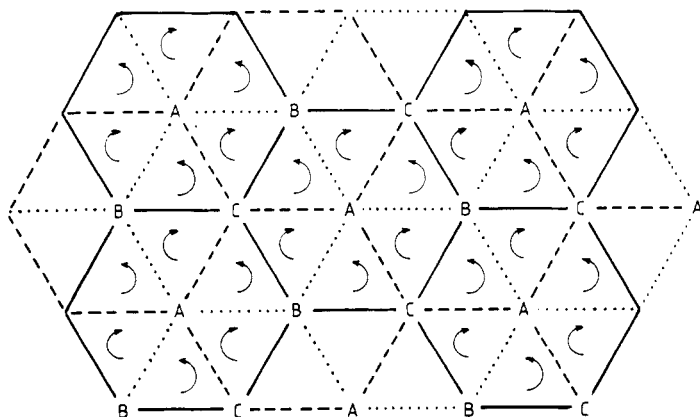


**Figure 17.** The postulated triple-honeycomb discommensurate structure for  $1T_2$ -TaS<sub>2</sub>, in which  $q_c^{(z)} = c_0^*/3$ . The domains appearing here have alternant handedness of their  $3c_0$  stack (Walker and Withers 1983). The discommensurations in this model give successive nodes that incorporate only two out of the three sandwiches per cell. This may account for their lack of visibility, contrasting with the weaker 2H CDW (figure 12), where every DC is active in every sandwich.

Yamamoto (1983) has analysed in detail the early unpublished x-ray results of Brouwer (1978) for the  $NC\ 1T_2$  phase at room temperature and has concluded that both the relative amplitudes between displacement harmonics and also their PLD eigenvector characteristics are indeed in close agreement with what is to be expected from an ideal sharply discommensurate, domain-like structure. It would accordingly be of great interest to have a detailed x-ray study of the relative amplitudes of the higher harmonics in the T phase, and in particular to see if harmonics induced by the  $3q_2 - q_3$  and  $3q_3 - q_1$  commensurability conditions have significant amplitude.

One would obviously like to obtain direct electron microscope imaging evidence of the above-indicated discommensurate domain structures. While a clear domain-like contrast is observable by satellite dark-field electron microscopy within the 'commensurate'  $1T_3$  phase (Fung *et al* 1980, Mutka *et al* 1984), no domain structure of the appropriate kind has yet been resolved within the  $NC\ 1T_2$  phase. High-resolution lattice imaging likewise has failed to produce direct evidence of the sought-for domain structure within the  $1T_2$  phase (Parsons 1976, Stobbs 1977, Van Tendeloo *et al* 1981, Iijima and Bando 1981, Steeds *et al* 1985). The resolution of this dilemma remains a matter of present concern.

Some of the problems are immediately apparent. The domains as deducible from  $\delta$  are quite small: they are only eight superlattice cells or 80 Å across. The fraction of cells within the DCs is therefore very considerable. Despite the small domain size, strong DC pinning as in 2H-TaSe<sub>2</sub> could furthermore render the domains rather irregular in shape. This would then impair the quality of the  $3c_0$  stack and hence the projection of the DCs onto the image plane. Actually the very sharpness of the observed  $c^*/3$  spotting may cast some doubt upon current interpretation of the nature of the stacking that is responsible. With the 2H materials, it should be recalled (see figure 12) that the DCs are observed to stack more or less vertically, i.e. the phase slip occurs in each sandwich at the same projected location (Wilson and Vincent 1984, Bird and Withers 1985, Wilson 1985b). Finally it should be remembered that the visibility of the 2H DC arrays is enormously enhanced by virtue of the orthorhombic phasing of the commensurate domains. XPS results (Hughes and Pollak 1976) remain, whatever the details might be, to seem to leave little doubt that  $1T_2$  must be as strongly discommensurate as 2H-TaSe<sub>2</sub>, in line with all current diffraction evidence. At this point by way of conclusion we return the reader to the abstract.

## Acknowledgments

We are very grateful for financial support from the SERC (RLW, post-doctoral fellowships) and the Royal Society (JAW, senior research fellowship) enabling us to conduct this work. We also thank our colleagues in the department for their interaction on these matters.

## References

- Anderson P W 1984 *Basic Notions of Condensed Matter Physics* (California: Benjamin-Cummings) p 99  
 Aubry S 1983 *J. Phys. C: Solid State Phys.* **16** 2497  
 Bak P 1982 *Rep. Prog. Phys.* **45** 587  
 Bak P, Coppersmith S, Shapir Y, Fishman S and Yeomans J 1985 *J. Phys. C: Solid State Phys.* **18** 3911  
 Barmatz M, Testardi L R and DiSalvo F J 1975 *Phys. Rev. B* **12** 4367

- Bernard L, Currat R, Delamoye P, Zeyen C M E, Hubert S and de Kouchkovsky R 1983 *J. Phys. C: Solid State Phys.* **16** 433
- Berthier C, Jérôme D and Molinie 1978 *J. Phys. C: Solid State Phys.* **11** 797
- Bird D M 1985 unpublished
- Bird D M, McKernan S and Steeds J W 1985 *J. Phys. C: Solid State Phys.* **18** 499
- Bird D M and Withers R L 1985 *J. Phys. C: Solid State Phys.* **18** 519
- Boswell F W, Prodan A and Brandon J K 1983 *J. Phys. C: Solid State Phys.* **16** 1067
- Brouwer R 1978 *PhD Thesis* University of Groningen, The Netherlands
- Brouwer R and Jellinek F 1980 *Physica B* **99** 51
- Bruce A D 1980 *Adv. Phys.* **29** 111
- Bruce A D and Cowley R A 1980 *Adv. Phys.* **29** 219
- Bruce A D, Murray A F and Cowley R A 1978 *J. Phys. C: Solid State Phys.* **11** 3577
- Bruce D A 1980 *J. Phys. C: Solid State Phys.* **13** 4615
- Bullett D W 1978 *J. Phys. C: Solid State Phys.* **11** 4501
- Butz T, Ebeling K-H, Hagn E, Saibene S, Zech E and Lerf A 1986a *Phys. Rev. Lett.* **56** 639
- Butz T, Saibene S and Lerf A 1986b *J. Phys. C: Solid State Phys.* **19** 2675
- Butz T, Vasquez and Lerf A 1979 *J. Phys. C: Solid State Phys.* **12** 4509
- Campagnoli C, Gustinetti A, Stella A and Tosatti E 1980 *Physica B* **99** 271
- Chan S K and Heine V 1973 *J. Phys. F: Met. Phys.* **3** 795
- Chapman L D and Colella R 1984 *Phys. Rev. Lett.* **52** 652
- Chen C H 1984 *Solid State Commun.* **49** 645
- Chen C H, Gibson J M and Fleming R M 1982 *Phys. Rev. Lett.* **52** 652
- Chevalier J P A A and Stobbs W M 1975 *Phil. Mag.* **31** 733
- Cowley R A 1980 *Adv. Phys.* **29** 1
- Craven R A and Meyer S F 1977 *Phys. Rev. B* **16** 4583
- DiSalvo F J 1977 *Electron-Phonon Interactions and Phase Transitions* ed. T Riste (New York: Plenum) p 107
- DiSalvo F J and Waszczak J V 1981 *Phys. Rev. B* **23** 457
- DiSalvo F J, Wilson J A, Bagley B G and Waszczak J V 1975 *Phys. Rev. B* **12** 2220
- Doran N J, Ricco B, Schrieber M, Titterington D J and Wexler G 1978a *J. Phys. C: Solid State Phys.* **11** 699
- Doran N J, Ricco B, Titterington D J and Wexler G 1978b *J. Phys. C: Solid State Phys.* **11** 685
- Doran N J and Woolley A M 1981 *J. Phys. C: Solid State Phys.* **14** 4257
- 1983 *J. Phys. C: Solid State Phys.* **16** L675
- Dugdale J S 1977 *Structures and Properties of Solids, The Electrical Properties of Metals and Alloys* vol 5, ed. B R Coles (New York: Arnold)
- Eaglesham D J 1985 *PhD Thesis* University of Bristol
- Eaglesham D J, Bird B, Withers R L and Steeds J W 1985a *J. Phys. C: Solid State Phys.* **18** 1
- Eaglesham D J, McKernan S and Steeds J W 1985b *J. Phys. C: Solid State Phys.* **18** L27
- Eaglesham D J, Withers R L and Bird D M 1986 *J. Phys. C: Solid State Phys.* **19** 359
- Edwards J and Frindt R F 1971 *J. Phys. Chem. Solids* **32** 2217
- Eibschutz M, Salomon D and DiSalvo F J 1983 *Phys. Lett.* **93A** 259
- 1986 unpublished
- Fehlner W R and Loly P D 1974 *Solid State Commun.* **14** 653
- Feldman J L 1982 *Phys. Rev. B* **25** 7132
- Fleming R M, Moncton D E, Axe J D and Brown G S 1984 *Phys. Rev. B* **30** 1877
- Fleming R M, Moncton D E and McWhan D B 1978 *Phys. Rev. B* **19** 5560
- Fleming R M, Moncton D E, McWhan D B and DiSalvo F J 1980 *Phys. Rev. Lett.* **45** 576
- Friedel J 1985 *Phil. Trans. R. Soc. A* **314** 189
- Friend R H and Jérôme D 1979 *J. Phys. C: Solid State Phys.* **12** 1441
- Fröhlich H 1954 *Proc. R. Soc. A* **223** 296
- Fung K K, McKernan S, Steeds J W and Wilson J A 1981 *J. Phys. C: Solid State Phys.* **14** 5417
- Fung K K, Steeds J W and Eades J A 1980 *Physica B* **99** 47
- Giuliani G F and Overhauser A W 1981 *Phys. Rev. B* **23** 373
- Haas C 1978 *Solid State Commun.* **26** 709
- 1979 *Current Topics in Materials Science* vol 3, ed. E Kaldis (Amsterdam: North Holland) pp 1–51
- Halperin B I and Rice T M 1968 *Solid State Phys.* **21** 115 (New York: Academic)
- Horowitz B, Gutfreund M and Weger M 1975 *Phys. Rev. B* **12** 3174
- Hughes H P and Pollak R A 1976 *Phil. Mag.* **34** 1025
- Huntley D J, DiSalvo F J and Rice T M 1978 *J. Phys. C: Solid State Phys.* **11** L767

- Iijima S and Bando Y 1981 *Proc. 39th Ann. EMSA Conf. 1981* ed. G W Bailey (Baton Rouge, LA: Claitors)
- Inglesfield J E 1980 *J. Phys. C: Solid State Phys* **13** 17
- Jacobs A E and Walker M B 1980 *Phys. Rev. B* **21** 4132
- Jericho M H, Simpson A M and Frindt R F 1980 *Phys. Rev. B* **22** 490
- Khanna S K, Pouget J P, Comès R, Garito A F and Heeger A J 1977 *Phys. Rev. B* **16** 1468
- Klipstein P C, Pereira C M and Friend R H 1984 *Physics and Chemistry of Electrons and Ions in Condensed Matter: Nato Advanced Study Inst.* (Cambridge) 1983 vol 130, ed. J V Acrivos, N F Mott and A D Yoffe (New York: Plenum) pp 549–59
- Kotani A and Harada I 1980 *J. Phys. Soc. Japan* **49** 535
- Littlewood P B and Heine V 1981 *J. Phys. C: Solid State Phys.* **14** 2943
- Littlewood P B and Rice T M 1982 *Phys. Rev. Lett.* **48** 44
- McKernan S, Steeds J W and Wilson J A 1982 *Phys. Scr.* **T 1** 74
- McMillan W L 1975a *Phys. Rev. B* **12** 1187
- 1975b *Phys. Rev. B* **12** 1197
- 1976 *Phys. Rev. B* **14** 1496
- 1982 unpublished
- McWhan D B, Axe J D and Youngblood R 1981 *Phys. Rev. B* **24** 5391
- McWhan D B, Fleming R M, Moncton D E and DiSalvo F J 1980 *Phys. Rev. Lett.* **45** 269
- Mahy J, van Landuyt J and Amelinckx S 1982 *Phys. Status Solidi* **A 74** K89
- 1984 *Mat. Res. Symp. Proc.* **22** 181
- Mahy J, Van Landuyt J, Amelinckx S, Uchida Y, Bronsema K D and van Smaalen G 1985 *Phys. Rev. Lett.* **55** 1188
- Marmeggi J C, Delapalme A, Lander G H, Vettier C and Lehner N 1982 *Solid State Commun.* **43** 577
- 1983 *Physica B* **120** 263
- Mattheiss L F 1973 *Phys. Rev. B* **8** 3719
- Monceau P 1985 *Electronic Properties of Inorganic Quasi 1-Dimensional Compounds* part II, ed. P Monceau (Dordrecht: Reidel) pp 139–268
- Moncton D E 1975 *PhD Thesis* MIT
- Moncton D E, Axe J D and DiSalvo F J 1977 *Phys. Rev. B* **16** 801
- Motizuki K and Ando E 1983 *J. Phys. Soc. Japan* **52** 2849
- Motizuki K, Kimura K, Ando E and Suzuki N 1984 *J. Phys. Soc. Japan* **53** 1078
- Mutka H and Housseau N 1982 *Phil. Mag B* **45** 361
- 1983 *Phil. Mag. A* **47** 797
- Mutka H, Housseau N, Pelissier J, Ayroles R and Roucau C 1984 *Solid State Commun.* **50** 161
- Mutka H, Zuppiroli L, Molinie P and Bourgoin J C 1981 *Phys. Rev. B* **23** 5030
- Myron H W, Rath J and Freeman A J 1977 *Phys. Rev. B* **15** 885
- Naito M, Nishihara H and Tanaka S 1985a *J. Phys. Soc. Japan* **52** 3946
- 1985b *Proc. 17th Conf. Semiconductors (Kyoto) 1984* p 1469
- Naito M and Tanaka S 1982 *J. Phys. Soc. Japan* **51** 219, 228
- Nakanishi K and Shiba H 1977 *J. Phys. Soc. Japan* **43** 1839
- 1978a *J. Phys. Soc. Japan* **45** 1147
- 1978b *J. Phys. Soc. Japan* **44** 1465
- 1983 *J. Phys. Soc. Japan* **52** 1278
- 1984 *J. Phys. Soc. Japan* **53** 1103
- Nakanishi K, Takatera H, Yamada Y and Shiba H 1977 *J. Phys. Soc. Japan* **43** 1509
- Nishihara H, Scholz G A, Naito M, Frindt R F and Tanaka S 1983 *J. Magn. Magn. Mater.* **31–4** 717
- Nuñez-Regueiro M, Lopez Castillo J and Ayache C 1985 *Phys. Rev. Lett.* **55** 1931
- Overhauser A W 1962 *Phys. Rev.* **128** 1437
- 1971 *Phys. Rev. B* **3** 3173
- Parsons J R 1976 *Proc. Microscopy Soc., Canada* **3** 22
- Peierls R E 1955 *Quantum Theory of Solids* (Oxford: OUP) p 108
- Pfeiffer L, Kovacs T and DiSalvo F J 1984 *Phys. Rev. Lett.* **52** 687
- Pfeiffer L, Walstedt R E, Bell R F and Kovacs T 1982 *Phys. Rev. Lett.* **44** 1455
- Pouget J P 1978 *Solid State Phase Transformations in Metals and Alloys* (Orsay: Les Editions de Physique) p 523
- Renker B and Comès R 1975 *Low Dimensional Cooperative Phenomena* ed. H J Keller (New York: Plenum) p 235
- Rice M J and Strässler S 1973 *Solid State Commun.* **13** 125

- Rice T M and Scott G K 1975 *Phys. Rev. Lett.* **35** 120
- Sahu D and Walker M B 1985 *Phys. Rev. B* **32** 1643
- Schmid P E 1976 *Festkörperprobleme* vol 16 (Braunschweig: Vieweg) p 47
- Scholz G A, Singh O, Frindt R F and Curzon A E 1982 *Solid State Commun.* **44** 1455
- Scruby C B, Williams P M and Parry G S 1975 *Phil. Mag.* **31** 255
- Shiba H and Nakanishi K 1986 *Structural Phase Transitions in LTMC* ed. K Motizuki (Dordrecht: Reidel) to appear
- Slough C G, McNairy W W, Coleman R V, Drake B and Hansma P K 1986 unpublished
- Smith H G and Lander G H 1984 *Phys. Rev. B* **30** 5407
- Smith N V, Kevan S D and DiSalvo F J 1985 *J. Phys. C: Solid State Phys.* **18** 3175
- Steeds J W, Bird D, Eaglesham D J, McKernan S, Vincent R and Withers R L 1985 *Ultramicroscopy* **18** 97
- Stiles J A R and Williams D L 1976 *J. Phys. C: Solid State Phys.* **9** 3941
- Stobbs W M 1977 *Phil. Mag.* **35** 1001
- Tanda S and Sambongi T 1985 *Synth. Met.* **11** 85
- Tanda S, Sambongi T, Tani T and Tanaka S 1984 *J. Phys. Soc. Japan* **53** 476
- Terasaki O 1982 *J. Phys. Soc. Japan* **51** 2159
- Tsutsumi K 1982 *Phys. Rev. B* **26** 5756
- Valic M I, Abdolali K and Williams D L 1975 *Proc. 18th Ampère Meeting (Nottingham) 1974* vol 2 p 369
- Van Landuyt J, Van Tendeloo G and Amelinckx S 1974 *Phys. Status Solidi a* **26** 359
- Van Tendeloo G, Van Landuyt J and Amelinckx S 1981 *Phys. Status Solidi a* **64** K105
- Varma C M and Simons A L 1983 *Phys. Rev. Lett.* **51** 138
- Varma C M and Weber W 1977 *Phys. Rev. Lett.* **39** 1094
- 1979 *Phys. Rev. B* **19** 6142
- Wakabayashi N, Smith H G and Nicklow R M 1975 *Phys. Rev. B* **12** 659
- Walker M B and Jacobs A E 1982 *Phys. Rev. B* **25** 4856
- Walker M B and Withers R L 1983 *Phys. Rev. B* **28** 2766
- Weber W 1980 *Physics of Transition Metals 1980* (Inst. Phys. Conf. Ser. 55) p 495
- Wexler G and Woolley A M 1976 *J. Phys. C: Solid State Phys.* **9** 1185
- Wilson J A 1977 *Phys. Rev. B* **15** 5748
- 1978 *Phys. Rev. B* **17** 3880
- 1982 *J. Phys. F: Met. Phys.* **12** 2469
- 1985a *Phil. Trans. R. Soc. A* **314** 159–77
- 1985b *J. Phys. F: Met. Phys.* **15** 591
- Wilson J A, DiSalvo F J and Mahajan S 1974 *Phys. Rev. Lett.* **32** 882
- 1975 *Adv. Phys.* **24** 117
- Wilson J A and Vincent R 1984 *J. Phys. F: Met. Phys.* **14** 23
- Wilson J A and Yoffe A D 1969 *Adv. Phys.* **18** 193
- Woolley A M and Wexler G 1977 *J. Phys. C: Solid State Phys.* **10** 2601
- Yamamoto A 1983 *Phys. Rev. B* **27** 7823
- Yoshida Y and Motizuki K 1982 *J. Phys. Soc. Japan* **51** 2107
- Ziebeck K R A, Dorner B, Stirling W G and Schöllhorn R 1977 *J. Phys. F: Met. Phys.* **7** 1139